© 2021. Published by The Company of Biologists Ltd | Development (2021) 148, dev192401. doi:10.1242/dev.192401

RESEARCH ARTICLE

Groucho co-repressor proteins regulate β cell development and proliferation by repressing *Foxa1* in the developing mouse pancreas

Alexandra Theis[1,‡], Ruth A. Singer[2,3,‡,*], Diana Garofalo[2], Alexander Paul[2,4], Anila Narayana[1] and Lori Sussel[1,2,§]

ABSTRACT

Groucho-related genes (GRGs) are transcriptional co-repressors that are crucial for many developmental processes. Several essential pancreatic transcription factors are capable of interacting with GRGs; however, the *in vivo* role of GRG-mediated transcriptional repression in pancreas development is still not well understood. In this study, we used complex mouse genetics and transcriptomic analyses to determine that GRG3 is essential for β cell development, and in the absence of *Grg3* there is compensatory upregulation of *Grg4*. *Grg3/4* double mutant mice have severe dysregulation of the pancreas gene program with ectopic expression of canonical liver genes and *Foxa1*, a master regulator of the liver program. *Neurod1*, an essential β cell transcription factor and predicted target of *Foxa1*, becomes downregulated in *Grg3/4* mutants, resulting in reduced β cell proliferation, hyperglycemia, and early lethality. These findings uncover novel functions of GRG-mediated repression during pancreas development.

KEY WORDS: Pancreas development, β cells, Groucho/TLE co-repressor, Foxa1, Mouse

INTRODUCTION

The pancreas is a multifunctional organ comprising exocrine and endocrine tissue. The exocrine tissue represents the majority of the organ and secretes digestive enzymes into the duodenum. The adult endocrine cell compartment is primarily composed of insulin-secreting β cells, glucagon-secreting α cells, somatostatin-secreting δ cells and pancreatic polypeptide-secreting PP cells that are clustered into discrete cellular bundles called the islets of Langerhans. Together, the islet endocrine cells secrete hormones to regulate glucose homeostasis. Dysfunction in this regulation results in diabetes mellitus, an increasingly prevalent disease worldwide characterized by hyperglycemia due to the inability to adequately respond to or secrete endogenous insulin (Cernea and Dobreanu, 2013; American Diabetes, 2020). Understanding the processes underlying normal pancreas development can inform mechanisms of dysfunction in diabetes and provide insights into developing β cell replacement therapies.

Pancreas organogenesis in the developing mouse begins between embryonic days (e) 8.5-9.0 when pancreatic duodenal homeobox $(PDX1)^+$ cells are specified from the foregut endoderm (Jorgensen et al., 2007). All functional cells of the adult pancreas are derived from a $PDX1^+$ multipotent progenitor population. As pancreas development progresses, a distinct neurogenin 3 $(NEUROG3)^+$ endocrine progenitor population arises, from which all pancreatic endocrine cells will be specified. Following endocrine specification, the maturation, expansion and organization of islet cells occurs throughout the rest of development and postnatally, resulting in the functional adult endocrine pancreas (Pan and Wright, 2011).

Development of the pancreas is controlled by a complex network of transcription factors that regulate gene expression with cellular and temporal specificity (Dassaye et al., 2016). Each of these factors has a unique repertoire of target genes that they can activate or repress. Often, the regulatory function of transcription factors relies on interactions with co-activators or co-repressors. One family of such co-repressors are encoded by the Groucho-related [GRG; also known as transducer-like enhancer of split (TLE)] genes. *groucho* was originally discovered in *Drosophila* and is conserved in mammals, which have four full-length GRG genes (Paroush, 1994; Buscarlet and Stifani, 2007; Turki-Judeh and Courey, 2012; Agarwal et al., 2015). There are also two truncated family members – GRG5 (the mouse ortholog of human AES; also known as TLE5) and GRG6 (TLE6) – that are thought to inhibit the function of full-length GRG proteins (Marcal et al., 2005; Zhang et al., 2008). GRG proteins are unable to bind DNA directly; instead, they are recruited to the genome by interactions with specific peptide motifs found in an array of transcription factors. The repressive function of GRGs is due in part to their ability to recruit histone deacetylases (HDACs) and the Polycomb repressive complex (PRC), which condense chromatin and prevent transcription of target genes (Chen et al., 1999; Papizan et al., 2011; Patel et al., 2012; Turki-Judeh and Courey, 2012).

GRGs are involved in many aspects of mammalian development and cellular functions, with each GRG having a unique tissue expression profile. Previous studies have identified crucial roles for GRGs in neurodevelopment, osteogenesis, hematopoiesis, adipogenesis and kidney development (Muhr et al., 2001; Cai et al., 2003; Villanueva et al., 2011; Wheat et al., 2014). Additionally, a study of embryonic pancreas explants from *Grg3* (*Tle3*) null mice demonstrated that endocrine cells failed to delaminate from the trunk epithelium and displayed defective differentiation *ex vivo* (Metzger et al., 2012). In an *in vitro* β cell model, GRG3 repressed expression of *Arx* and glucagon to promote monohormonal β cell identity (Metzger et al., 2014). Together, these studies suggest there is a crucial role for

[1]Department of Pediatrics and Cell & Developmental Biology, Barbara Davis Center for Diabetes, University of Colorado Anschutz Medical Campus, Aurora, CO 80045, USA. [2]Department of Genetics and Development, Columbia University Medical Center, New York, NY 10032, USA. [3]Integrated Program in Cellular, Molecular and Biomedical Studies, Columbia University Medical Center, New York, NY 10032, USA. [4]Graduate program in Genetics and Development, Columbia University Medical Center, New York, NY 10032, USA.
‡These authors contributed equally to this work
*Present address: Laboratory of Molecular Neuro-Oncology, The Rockefeller University, New York, NY 10065, USA.

§Author for correspondence (lori.sussel@ucdenver.edu)

L.S., 0000-0003-4672-7304

Handling Editor: Samantha Morris
Received 7 May 2020; Accepted 24 February 2021

Development (2021) 148, dev192401. doi:10.1242/dev.192401

GRG3 during pancreas development; however, the analyses were limited by short time survival of the explants and caveats associated with β cell lines.

There are several known interacting partners of GRGs that have been characterized in different tissue contexts, including members of the HES, FOXA, NKX and PAX families of transcription factors, which also represent essential factors that regulate pancreas development (Eberhard et al., 2000; Muhr et al., 2001; Yao et al., 2001; Milili et al., 2002; Iype et al., 2004; Linderson et al., 2004; Sekiya and Zaret, 2007; Jangal et al., 2014). For example, HES1 promotes differentiation of the non-endocrine pancreas progenitor population, and FOXA1 and FOXA2 are expressed in the foregut endoderm from which the pancreas and liver are derived (Ang et al., 1993; Monaghan et al., 1993; Jensen et al., 2000; Kaestner, 2010). Whereas *Foxa1* transcript is primarily associated with the liver lineage and cannot be detected in early stage pancreatic tissue (Krentz et al., 2018; Li et al., 2018), *Foxa2* remains expressed in the pancreas lineage and FOXA2 induces early expression of PDX1 (Gao et al., 2008). Later in development, FOXA2 promotes endocrine differentiation and β cell function (Gao et al., 2010). Furthermore, PAX4 and PAX6 regulate the β/δ and β/α cell fates, respectively, and NKX2-2 and NKX6-1 are necessary for endocrine cell differentiation and maintenance of β cell identity (Sander et al., 1997; Sosa-Pineda et al., 1997; St-Onge et al., 1997; Sussel et al., 1998; Collombat et al., 2003, 2005; Henseleit et al., 2005; Taylor et al., 2013; Gutierrez et al., 2017). In the context of pancreas development, we have previously shown that the interaction between NKX2-2 and GRG3 is necessary to prevent β-to-α cell reprogramming by repressing the α cell master regulatory gene, *Arx* (Papizan et al., 2011).

To characterize the role of GRGs in pancreas development more comprehensively, we determined that *Grg2* (*Tle2*) and *Grg3* were the two family members predominantly expressed during pancreas development, which corresponds with previously published expression data of the developing pancreatic epithelium (Hoffman et al., 2008). Surprisingly, mice with global deletion of *Grg2* had no discernable phenotype. Furthermore, pancreas-specific deletion of *Grg3* or a combination of *Grg2* and *Grg3* had surprisingly mild phenotypes. Pancreas-specific deletion of *Grg3 in vivo* also did not exhibit many of the previously reported phenotypes seen in pancreatic explants and cell culture models (Metzger et al., 2012, 2014). Remarkably, expression analysis revealed that in the absence of *Grg3*, *Grg4* (*Tle4*), the family member that is normally not expressed in the pancreas, is highly upregulated. Combined pancreatic deletion of *Grg3* and *Grg4* resulted in an exacerbated pancreas developmental phenotype and had significantly reduced numbers of β cells embryonically and perinatally, demonstrating that *Grg4* upregulation can partially compensate for loss of *Grg3*. At the molecular level, we determined that GRG activity was essential for repressing *Foxa1* expression. In the absence of *Grg3* and *Grg4*, *Foxa1* becomes erroneously expressed, resulting in downregulation of *Neurod1* and causing defects in β cell expansion, a phenotype similar to that seen in mice lacking *Neurod1* in the pancreas and β cells (Naya et al., 1997; Romer et al., 2019). Taken together, these findings provide new insights into the necessity of GRG transcriptional co-factors in pancreas organogenesis.

RESULTS

Grg3 is highly expressed in the embryonic pancreas and adult islets

Each member of the family of mammalian GRGs has a unique tissue-expression profile (Agarwal et al., 2015). To determine which GRGs are expressed in the pancreas in the absence of appropriate antibodies specific for each of the GRG proteins, we performed RNA *in situ* hybridization on embryonic tissue from wild-type mice, using probes for *Grg1-4* as well as *Pdx1* to delineate the developing pancreas (Fig. 1A). At both e13.5 and e15.5, epithelial *Grg1* expression could not be detected above background signal; however, *Grg2* and *Grg3* expression extensively overlapped with *Pdx1* (Fig. 1A). *Grg4* expression could be detected in the pancreatic mesenchyme at e13.5 but was no longer present at e15.5 (Fig. 1A). Because expression of the different GRG family members differed from previously published data (Hoffman et al., 2008), we also analyzed existing RNA-sequencing (RNA-seq) data for GRG gene expression. In sorted NEUROG3^{+} (NEUROG3-EGFP) endocrine progenitors from e15.5 pancreata, we confirmed expression of *Grg2* and *Grg3* in the pancreatic endocrine progenitor compartment, with *Grg3* being the most highly expressed *Groucho* family member (Fig. 1B, white bars). RNA-seq data from islets isolated from 4- and 12-week-old mice show that *Grg3* levels remained high in the endocrine population through adulthood (Fig. 1B), whereas *Grg1* and *Grg2* were both upregulated in adult islets (Gutierrez et al., 2017; Romer et al., 2019). Several published single-cell RNA-seq datasets also confirm these expression patterns (Scavuzzo et al., 2018; Tabula Muris Consortium, 2018). Based on these results, we focused our analyses of embryonic pancreas-specific GRG function on *Grg2* and *Grg3*.

Pancreas-specific loss of *Grg3* leads to hyperglycemia and upregulation of *Grg4*

Because genetic disruption of *Grg2* has not been previously performed in mice, we generated mice carrying a null mutation of *Grg2* using a *Grg2/Tle2*$^{tm1(KOMP)Vlcg}$ embryonic stem cell line (Fig. 1C,D). Surprisingly, given the severe phenotypes associated with global knockout of *Grg3* (embryonic lethality due to placental defects) or *Grg4* (lethality around 4 weeks of age due to hematopoietic and bone development defects), the *Grg2* homozygous null mice lived into adulthood with no apparent defects (Villanueva et al., 2011; Gasperowicz et al., 2013; Wheat et al., 2014). These mice were euglycemic and did not appear to have any overt pancreatic islet phenotypes (Fig. 1E,F).

Owing to the embryonic lethality associated with a global deletion of *Grg3* (Gasperowicz et al., 2013), we generated pancreas-specific *Grg3* mutants using *Pdx1:Cre* to drive recombination of a floxed *Grg3* allele (*Pdx1:Cre; Grg3*$^{fl/fl}$) (Hingorani et al., 2003; Villanueva et al., 2011) (Fig. S1A,B). Previous analysis of embryonic pancreas explants derived from *Grg3*$^{-/-}$ mice suggested that *Grg3* was essential for the appropriate differentiation of all pancreatic endocrine cells (Metzger et al., 2012). Based on these previous findings, we anticipated that the *Pdx1:Cre; Grg3*$^{fl/fl}$ mice would be neonatal lethal, and therefore assessed the phenotype of *Pdx1:Cre; Grg3*$^{fl/fl}$ embryos just prior to birth. Surprisingly, at e18.5, the *Pdx1:Cre; Grg3*$^{fl/fl}$ islets appeared remarkably normal, exhibiting only a trend in decreased β cell numbers (Fig. 2A,B). Consistent with the immunofluorescence data, there was a small, but significant, decrease in *Ins1*, *Ins2* and *Gcg* mRNA expression in e18.5 pancreata (Fig. 2C). There were no apparent defects in the number of non-β endocrine cells or levels of the other endocrine hormones at this stage (Fig. 2A-C), although we were able to detect a small number of insulin (INS) and somatostatin (SST) co-expressing cells in adult islets (Fig. S1C).

Previous work suggested that the defect in endocrine cell differentiation was due to defects in the suppression of E-cadherin (cadherin 1) (Metzger et al., 2012). However, consistent with our observation that there were no general defects in the formation of the non-β endocrine cell lineages at e16.5, nor any observable delamination

Development (2021) 148, dev192401. doi:10.1242/dev.192401

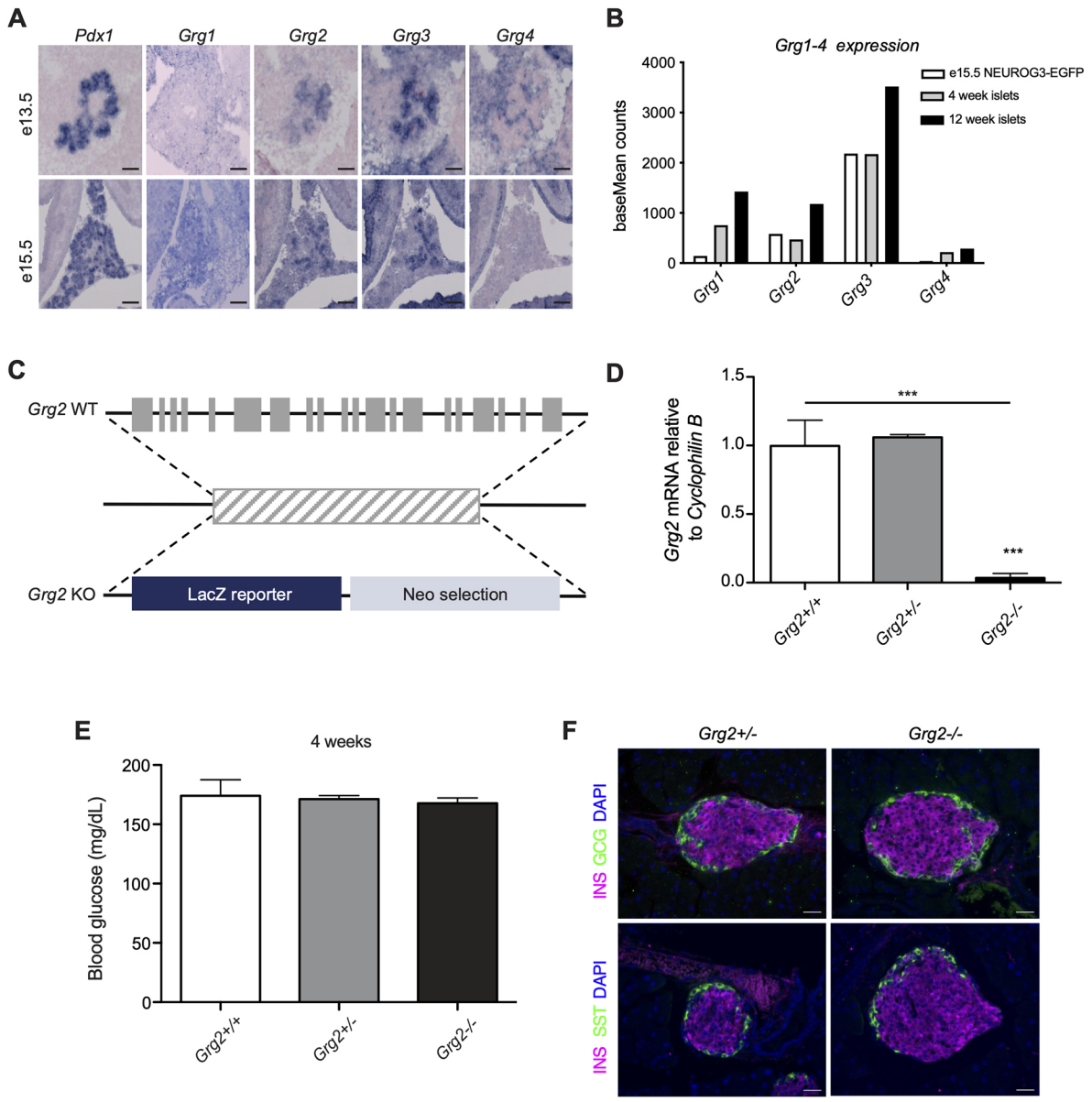

Fig. 1. *Grg3* is highly expressed in the embryonic pancreas and adult islets. (A) *Grg2* and *Grg3* expression overlaps with pancreatic *Pdx1* expression at e13.5 and e15.5. *Grg4* is expressed in the mesenchyme surrounding the pancreas at e13.5. Scale bars: 100 µm. (B) baseMean counts from previously published RNA-seq experiments. *Grg3* is highly expressed in sorted NEUROG3^{+} endocrine progenitor cells at e15.5 and remains expressed in isolated adult islets at 4 weeks and 12 weeks. (C) Schematic of *Grg2* knockout (KO) allele. (D) RT-qPCR validation of *Grg2* knockout showing loss of transcript in P0 *Grg2*$^{-/-}$ homozygous pancreata. *n*=4-7 for all genotypes. ***$P\leq0.0001$; two-tailed Student's *t*-test. (E) *Ad libitum* blood glucose measurements of 4-week-old *Grg2*$^{-/-}$ mice. *n*=4-6 for all genotypes. (F) Immunofluorescence analysis of 6-week-old *Grg2* heterozygous and homozygous mutants showing no visible islet phenotype. Scale bars: 25 µm.

defects, we could not detect increased expression of E-cadherin mRNA in the *Pdx1:Cre; Grg3*$^{fl/fl}$ mutants (Fig. 2C, Fig. S1D).

In light of the subtle defects observed in the *Pdx1:Cre; Grg3*$^{fl/fl}$ embryos, we next assessed the phenotype of postnatal mutant animals. *Pdx1:Cre; Grg3*$^{fl/fl}$ mice were born at normal Mendelian ratios; however, they were hyperglycemic compared with control littermates at all time points tested (Fig. 2D). At 6 weeks of age, *Pdx1:Cre; Grg3*$^{fl/fl}$ mice displayed impaired glucose clearance (Fig. 2E,F). Consistent with this, immunofluorescent analysis of *Pdx1:Cre; Grg3*$^{fl/fl}$ islets isolated from 6-week-old mice revealed a discernable decrease in the number of β cells, with no apparent effect on the other endocrine cell types (Fig. 2G). Consistent with the decreased number of β cells, lower levels of *Ins1* and *Ins2* genes, and impaired glucose clearance, islets isolated from 12-week-old *Pdx1:Cre; Grg3*$^{fl/fl}$ mice also had decreased intracellular insulin content (Fig. 2H).

Overall, the observed *Pdx1:Cre; Grg3*$^{fl/fl}$ phenotype was not as severe as expected based on the previous knockout studies and the known functional interactions of GRG3 with NKX2-2 and other essential islet transcription factors (Buscarlet and Stifani, 2007; Jennings and Ish-Horowicz, 2008; Papizan et al., 2011; Metzger et al., 2012; Agarwal et al., 2015). The embryonic expression pattern of *Grg2* (Fig. 1A,B) suggested a possible functional redundancy between *Grg2* and *Grg3* that might compensate for the lack of *Grg3* expression in the pancreas. To test this, we intercrossed the *Grg2*$^{-/-}$ and *Pdx1:Cre; Grg3*$^{fl/fl}$ mice to generate *Grg2/3*

Development (2021) 148, dev192401. doi:10.1242/dev.192401

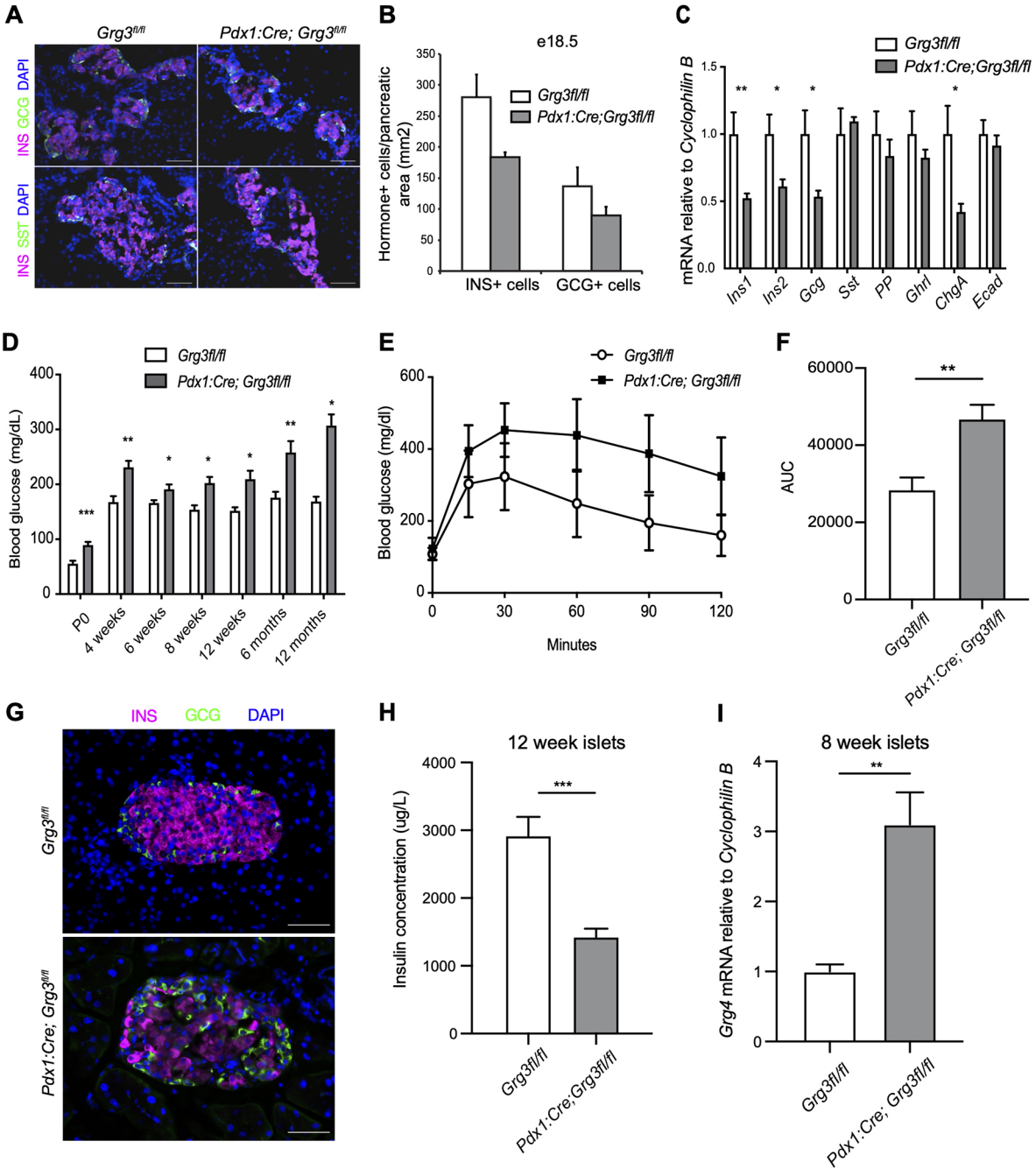

Fig. 2. Pancreas-specific loss of *Grg3* results in hyperglycemia, impaired glucose tolerance and upregulation of *Grg4*. (A) Immunofluorescence analysis of islet hormones insulin (INS) and glucagon (GCG) in e18.5 pancreata from control and *Pdx1:Cre; Grg3*$^{fl/fl}$ embryos. Scale bars: 50 µm. (B) Quantification of hormone^{+} cells from the experiment shown in A. *n*=3 for each genotype. (C) RT-qPCR analysis of islet hormones, chromogranin A (*ChgA*) and E-cadherin (*Ecad*) in e18.5 whole pancreata. *n*=3-4 for each genotype. **P*≤0.05, ***P*≤0.01; Student's two-tailed *t*-test. (D) Conditional loss of *Grg3* in the pancreas results in elevated *ad libitum* blood glucose levels at all time points between P0 and 12 months. *n*=3-10 for each time point. **P*≤0.05, ***P*≤0.01, ****P*≤0.001; two-tailed Student's *t*-test. (E) *Pdx1:Cre; Grg3*$^{fl/fl}$ mice are glucose intolerant at 6 weeks of age. *n*=13-19 for each genotype. (F) Area under the curve (AUC) calculations for the data shown in E. ***P*≤0.01; two-tailed Student's *t*-test. (G) Immunofluorescence staining of INS and GCG of 6-week-old islets show fewer INS^{+} β cells in *Pdx1:Cre; Grg3*$^{fl/fl}$ islet. Scale bars: 50 µm. (H) Intracellular insulin content of isolated islets from 12-week-old mice as measured with an insulin ELISA assay. *n*=3 for each genotype. ****P*≤0.001; two-tailed Student's *t*-test. (I) RT-qPCR analysis of *Grg4* mRNA expression in isolated islets from control and *Pdx1:Cre; Grg3*$^{fl/fl}$ 8-week-old animals. *n*=3.***P*≤0.01; Student's two-tailed *t*-test.

double-mutant mice; however, there was no worsening of the *Grg3* single mutant phenotype in the *Grg2/3* double-mutant mice (Fig. S2). Although *Grg1* and *Grg4* are not normally expressed in the developing endocrine pancreas, it was also possible that one or both of these family members became upregulated in response to deletion of *Grg3*; indeed, we observed a 3-fold increase in *Grg4* expression in isolated *Pdx1:Cre; Grg3*$^{fl/fl}$ islets (Fig. 2I), whereas *Grg1* was not significantly altered. This discovery led us to hypothesize that *Grg4* upregulation was compensating for the loss of *Grg3* and preventing a more severe pancreas phenotype.

Development (2021) 148, dev192401. doi:10.1242/dev.192401

Grg3/4 double mutants are extremely hyperglycemic with a reduction in β cells

To determine whether the upregulation of *Grg4* functionally compensates for the loss of *Grg3* in the *Pdx1:Cre; Grg3$^{fl/fl}$* mutants, we next generated *Grg3; Grg4* double knockout mice. Because the *Grg4* null mutation results in lethality around 4 weeks of age owing to bone and hematopoiesis defects, we obtained a floxed allele of *Grg4* and generated pancreas-specific *Grg3/Grg4* mutant mice (*Pdx1:Cre; Grg3/4*) (Wheat et al., 2014). Unlike the single *Pdx1:Cre; Grg3$^{fl/fl}$* mutants, we observed fewer than expected double knockout mice at weaning (12% versus 25%, χ^2 test, 10 litters, n=96, P=0.0193), suggesting that simultaneous deletion of *Grg3* and *Grg4* caused early postnatal lethality and confirming that upregulation of *Grg4* could partially compensate for lack of *Grg3*. The small number of double mutant mice that did survive to weaning, likely as a result of inefficient deletion of both *Grg3* and *Grg4* alleles, had normal body weight compared with *Pdx1:Cre* controls and *Pdx1:Cre; Grg3$^{fl/fl}$* single mutants (Fig. 3A). However, double *Grg3/4* mutants displayed more severe hyperglycemia and glucose intolerance phenotypes compared with *Pdx1:Cre; Grg3$^{fl/fl}$* mice (Fig. 3B-D). Along with having disorganized islet morphology, we also observed a small number of INS and SST co-expressing cells, similar to observations in *Pdx1:Cre; Grg3$^{fl/fl}$* mice (Fig. 3E). INS$^+$/GCG$^+$ cells were not observed in either the single or double knockout animals.

Because of the loss of most *Pdx1:Cre; Grg3/4* double knockout mice by weaning, we wanted to assess whether mice lacking both *Grg3* and *Grg4* alleles survived through gestation. We analyzed mice at postnatal day (P) 2 and found that *Pdx1:Cre; Grg3/4* double mutants were born at normal Mendelian ratios. Mutants showed no difference in body weight or general pancreas area, but already displayed elevated blood glucose levels as neonates (Fig. 4A-C), suggesting a possible defect in β cell development. Immunofluorescence analysis of islet hormone expression identified a significant reduction in the number of INS$^+$ cells, without apparent alterations in SST$^+$ or GCG$^+$ cells, indicating that the loss of *Grg3* and *Grg4* only affected development of the β cell lineage, although to a more severe extent than loss of *Grg3* alone (Fig. 4D,E).

To determine whether the decrease in β cell numbers was due to a defect in the formation of β cells during embryogenesis, we quantified the islet hormone-positive areas of e16.5 *Pdx1:Cre; Grg3/4* double knockout embryos. We found that although INS$^+$ β cells were specified by this stage, the overall INS$^+$ area was significantly smaller in the double mutant embryos, with no apparent changes in GCG- or SST-expressing cells (Fig. 4F,G). This did not appear to be associated with a decrease in the endocrine progenitor pool as we did not observe reduced numbers of NEUROG3-expressing endocrine progenitor cells (Fig. S3), consistent with previous reports that *Grg3* is expressed downstream of *Neurog3* (Metzger et al., 2012).

Pancreas genes are downregulated in *Grg3/4* mutant pancreata with ectopic expression of liver genes and the master liver regulator *Foxa1*

Our data revealed that β cells were being specified from the endocrine progenitor population, but there was decreased β cell mass at e16.5 and P2. Although the reduction in β cell numbers was significant, it was not sufficient to explain the resulting in perinatal hyperglycemia (Fig. 4). This led us to hypothesize that the remaining β cells were also dysfunctional due to developmental and/or maturation defects. To understand what was occurring in *Pdx1:Cre; Grg3/4* mutant pancreata after β cell formation but prior to birth (to avoid the many changes associated with the transition to milk-feeding), we performed transcriptomic analyses on e18.5 pancreata from *Pdx1:Cre; Grg3$^{fl/fl}$*, *Pdx1:Cre; Grg3/4* and *Pdx1:Cre* control embryos. DESeq2 analysis between the single mutant and control pancreata identified 1181 significantly differentially expressed genes, whereas double mutant and control pancreata had 1973 significant differentially expressed genes with 1007 upregulated and 966 downregulated genes (Fig. S4, Fig. 5A). Similar gene expression changes were observed in both the single and double mutant datasets, although the levels of gene expression changes were more severe in the *Pdx1:Cre; Grg3/4* double-mutant mice (Fig. S4).

Using PANTHER gene ontology (GO) software on the list of significantly downregulated genes, we found multiple pancreatic processes to be perturbed in the *Pdx1:Cre; Grg3/4* mutant pancreata (Fig. 5B, top section). Insulin secretion, zinc ion transmembrane transport and cAMP-mediated signaling, both essential components involved in insulin secretion, were among the top 5 GO terms identified. Genes encoding multiple islet hormones were also downregulated, including *Ins1*, *Ins2*, *Npy*, *Pyy* and *Ppy* (Fig. 5C), whereas *Gcg* and *Sst* were unchanged, consistent with our immunofluorescence analysis (Fig. 4D-G). In addition to GO terms associated with islet function, downregulated genes were also significantly associated with pancreas and endocrine pancreas development (Fig. 5B, top section), including *Foxa2*, *Pdx1*, *Neurod1* and *Pax6* (Fig. 5C). These gene expression changes could be explained by the decreased insulin area observed in e16.5 and P2 mutant pancreata (Fig. 4D-G), but could also be attributed to alterations in β cell function. Although the acinar and ductal tissues in *Pdx1:Cre; Grg3/4* mutants appeared normal, a small subset of acinar and ductal genes were downregulated, suggesting that loss of Grg3/4 could have subtle effects on exocrine functions (Fig. S5).

GRGs act primarily as transcriptional co-repressors, suggesting that these downregulated genes are likely an indirect consequence of defective upstream GRG-mediated gene repression. To identify genes that were more likely to be directly linked to loss of GRG function, we focused on genes that were significantly upregulated in *Pdx1:Cre; Grg3/4* mutant pancreata. Surprisingly, GO analysis of these genes revealed enrichment of metabolic processes normally found in the liver, including glycogen biosynthesis and metabolism, glucan metabolism, and polysaccharide metabolism (Fig. 5B, bottom section). Consistent with this, most of the genes with the highest fold changes were canonical liver genes (Fig. 5D), including the transcription factor *Foxa1*, which acts with *Foxa2* as major regulators of hepatocyte differentiation (Lee et al., 2005).

Foxa1 is expressed in the early foregut endoderm from where the pancreas and liver are both derived. During normal development, *Foxa1* expression diminishes in the pancreas and becomes restricted to the liver lineage (Li et al., 2018; Scavuzzo et al., 2018). In e18.5 *Pdx1:Cre; Grg3/4* mutants, *Foxa1* RNA expression was increased 8.7-fold (Fig. 5D). To determine whether ectopic FOXA1 could also be detected at the protein level, we used immunofluorescence to assess FOXA1 protein expression at e12.5, P2 and 6 weeks of age. Consistent with increased expression at the RNA level, FOXA1 protein could be detected in the pancreas of *Pdx1:Cre; Grg3/4* mutants at all ages tested (Fig. 5E, Fig. S6). In addition to FOXA1 protein expression, predicted *Foxa1* target genes were also significantly dysregulated in the *Pdx1:Cre; Grg3/4* mutant pancreata. Of the significantly differentially expressed genes, we identified 102 predicted *Foxa1* targets, of which 53 were upregulated and 49 were downregulated, in agreement with *Foxa1* being both an activator and repressor of gene expression (Fig. 5A, white dots; Table S1).

In addition to confirming the ectopic expression of FOXA1, we also sought to confirm expression of the liver genes identified by

Development (2021) 148, dev192401. doi:10.1242/dev.192401

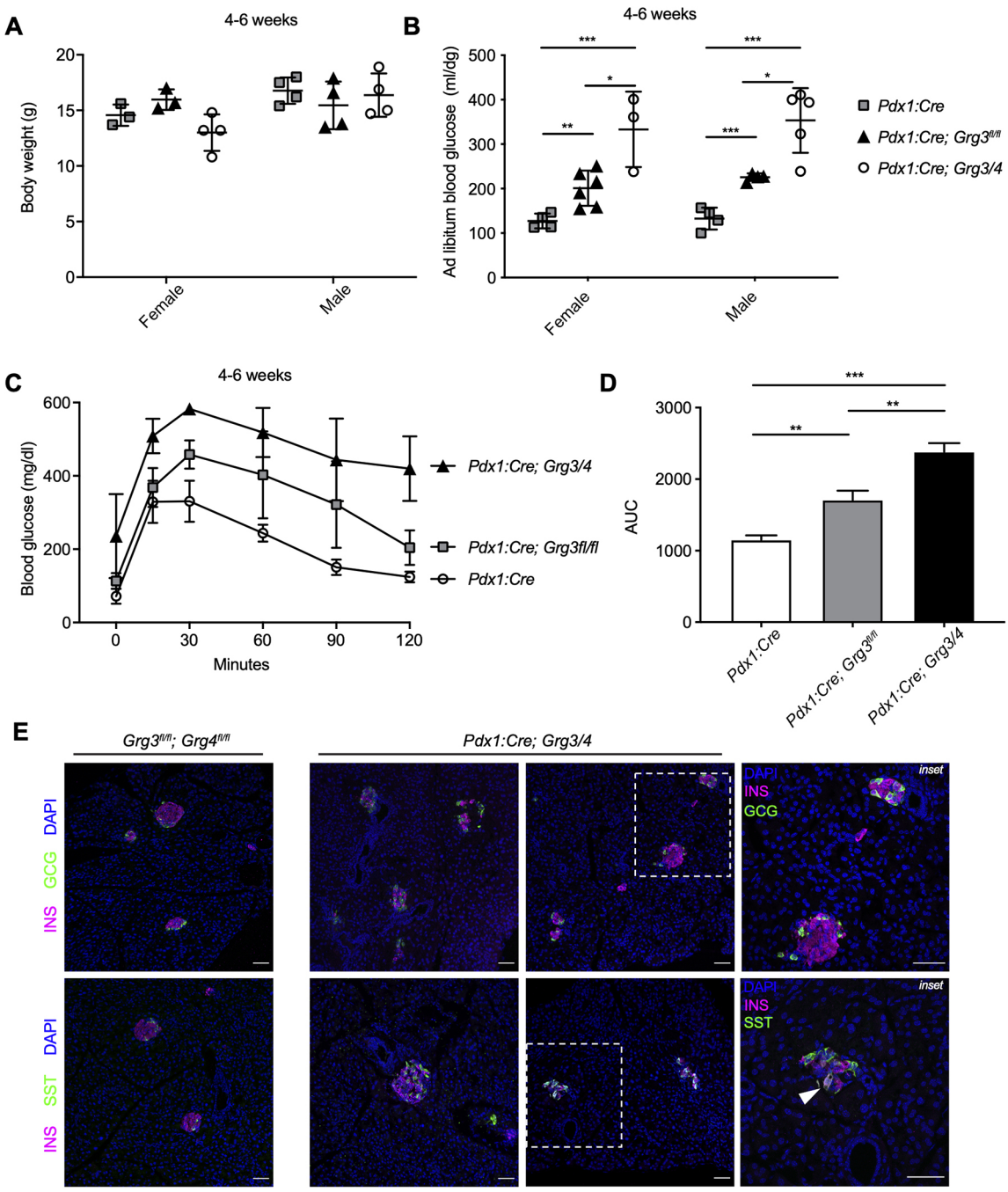

Fig. 3. *Pdx1:Cre; Grg3/4* mutants that survive to weaning age are extremely hyperglycemic with fewer β cells and bihormonal INS$^+$/SST$^+$ cells. (A) Body weight measurements of control and *Pdx1:Cre; Grg3/4* young adults show no difference between genotypes. *n*=3-4 for each genotype. (B) *Ad libitum* blood glucose measurements of 4- to 6-week-old mice showing hyperglycemia in *Pdx1:Cre; Grg3/4* double mutants compared with both *Pdx1:Cre* control and *Pdx1:Cre; Grg3$^{fl/fl}$* animals. *n*=3-6 for each genotype.*$P\leq0.05$; **$P\leq0.01$; ***$P\leq0.0001$; two-tailed Student's *t*-test. (C) Glucose tolerance tests of 4- to 6-week-old *Pdx1:Cre* control mice and *Pdx1:Cre;Grg3* and *Pdx1:Cre;Grg3/4* mutants. *n*=3-5 for each genotype. (D) AUC of the data shown in C showing increased AUC of *Grg3/4* double mutants compared with *Pdx1:Cre* control and *Grg3* single mutants. **$P\leq0.01$, ***$P\leq0.001$; two-tailed Student's *t*-test. (E) Immunofluorescence staining of islets from 4-week-old control and *Pdx1:Cre; Grg3/4* mutant mice showing a visible decrease in INS$^+$ β cells and disorganized islet morphology. Right-hand panels are magnifications of the boxed areas showing examples of INS$^+$SST$^+$ bihormonal cells in *Pdx1:Cre; Grg3/4* mutant. Arrowhead indicates INS$^+$SST$^+$ bihormonal cell. Scale bars: 50 µm.

RNA-seq. Although we were able to detect robust expression of a candidate liver gene *Serpina1e* mRNA (Fig. 5F), expression of SERPINA1A-E protein (also known as alpha1 antitryspin, AAT), could only be detected in very few cells in the *Pdx1:Cre; Grg3/4* mutant pancreata at e16.5 (Fig. 5G). This suggests that although liver genes were upregulated, they could not be translated. Dysregulation of the liver gene expression program did not influence pancreas patterning or overall pancreas morphology (Fig. S4B).

Neurod1 expression is lost in *Grg3/4* mutant β cells with a reduction in β cell proliferation

One of the predicted *Foxa1* targets that was downregulated in *Pdx1:Cre; Grg3/4* mutant pancreata was *Neurod1*. NEUROD1 is a

Development (2021) 148, dev192401. doi:10.1242/dev.192401

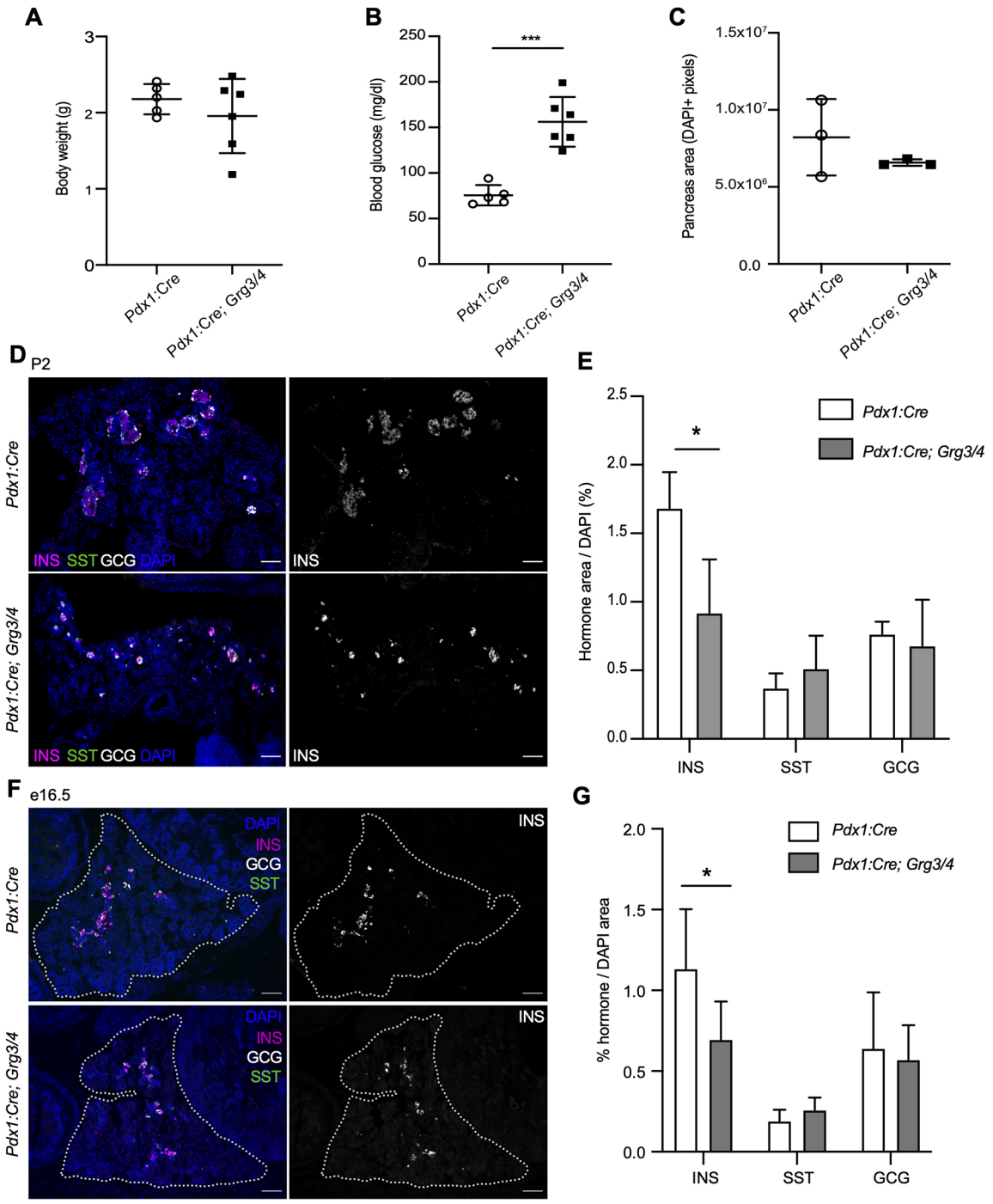

Fig. 4. Loss of *Grg3* and *Grg4* leads to perinatal hyperglycemia and a decrease in β cell area at P2 and e16.5. (A) Pancreas-specific knockout of *Grg3* and *Grg4* (*Pdx1:Cre; Grg3/4*) does not result in body weight changes in P2 mice. *n*=6. (B) *Pdx1:Cre; Grg3/4* mice have elevated blood glucose levels at P2 compared with *Cre*-only controls. *n*=6. ***$P \leq 0.0001$; two-tailed Student's *t*-test. (C) Pancreas area as measured by DAPI immunofluorescence is unchanged in *Pdx1:Cre; Grg3/4* mice at P2. *n*=3. Representative images are shown in D. (D) Immunofluorescence staining of P2 pancreata for INS, SST and GCG. Scale bars: 100 µm. (E) Quantification of hormone area relative to pancreas area (DAPI). *Pdx1:Cre; Grg3/4* mice have decreased INS^+ area with no changes in SST or GCG area. *n*=3-4 for each genotype. *$P \leq 0.05$; two-tailed Student's *t*-test. (F) Immunofluorescence staining of e16.5 pancreata for INS, SST and GCG. Dotted line delineates the pancreas. Scale bars: 50 µm. (G) Quantification of $hormone^+$ area relative to pancreas (DAPI) area as shown in F. *n*=6 for each genotype. *$P \leq 0.05$; two-tailed Student's *t*-test.

transcription factor required for β cell proliferation, survival and maturation (Naya et al., 1997; Gu et al., 2010; Romer et al., 2019). Interestingly, *Pdx1:Cre; Grg3/4* mutant β cells lacked expression of NEUROD1 (Fig. 6A, white arrowheads), whereas all β cells in control pancreata co-stained for insulin and NEUROD1. INS^-/NEUROD1+ cells likely represent non- β endocrine cells as previously described (Chao et al., 2007). Additionally, we found that many of the direct *Neurod1* target genes were significantly downregulated in *Pdx1:Cre; Grg3/4* mutant pancreata (Romer et al., 2019) (Fig. 6B). *Neurod1*$^{-/-}$ mice fail to form pancreatic islets and

Development (2021) 148, dev192401. doi:10.1242/dev.192401

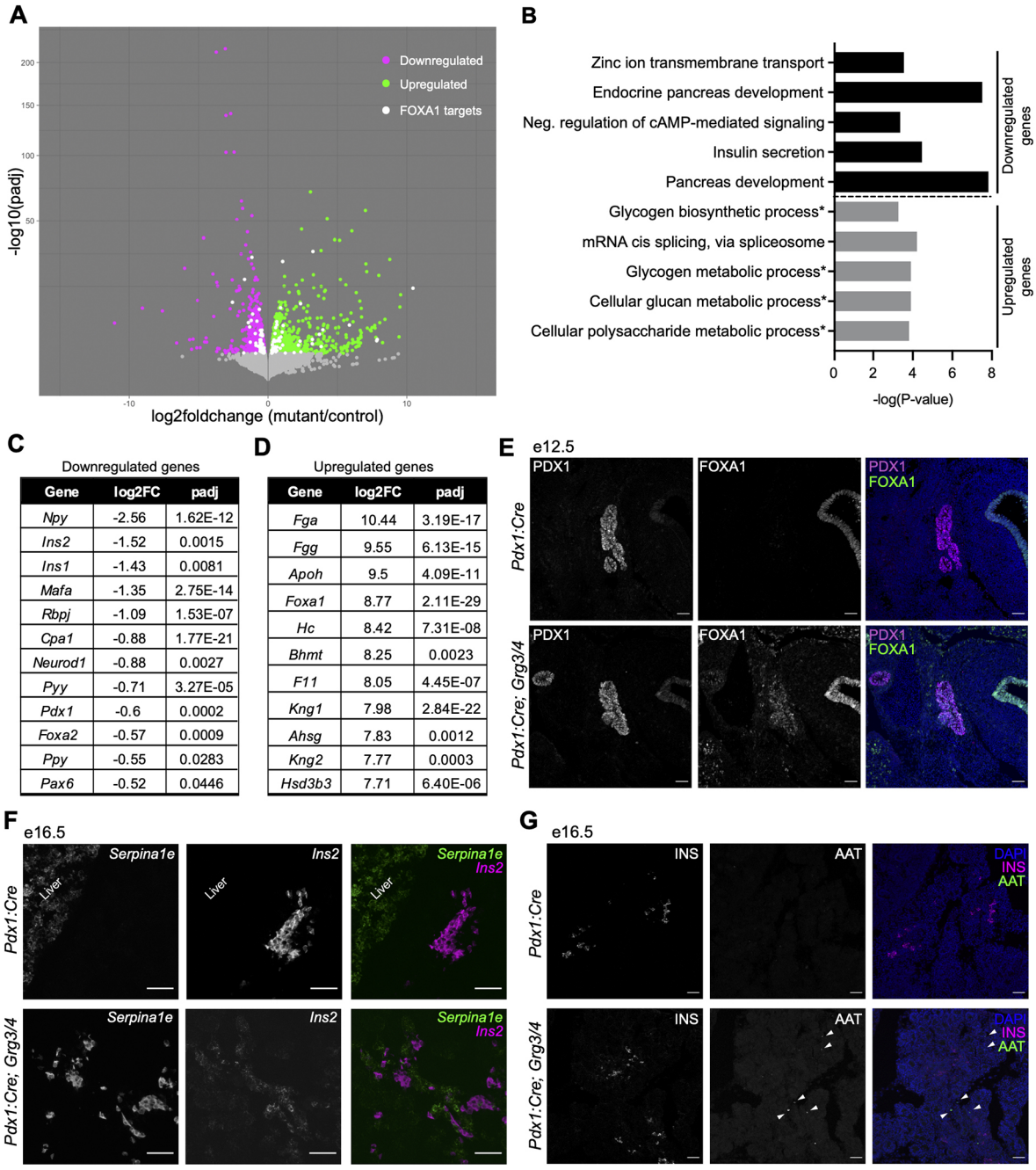

Gene	log2FC	padj
Npy	-2.56	1.62E-12
Ins2	-1.52	0.0015
Ins1	-1.43	0.0081
Mafa	-1.35	2.75E-14
Rbpj	-1.09	1.53E-07
Cpa1	-0.88	1.77E-21
Neurod1	-0.88	0.0027
Pyy	-0.71	3.27E-05
Pdx1	-0.6	0.0002
Foxa2	-0.57	0.0009
Ppy	-0.55	0.0283
Pax6	-0.52	0.0446

Gene	log2FC	padj
Fga	10.44	3.19E-17
Fgg	9.55	6.13E-15
Apoh	9.5	4.09E-11
Foxa1	8.77	2.11E-29
Hc	8.42	7.31E-08
Bhmt	8.25	0.0023
F11	8.05	4.45E-07
Kng1	7.98	2.84E-22
Ahsg	7.83	0.0012
Kng2	7.77	0.0003
Hsd3b3	7.71	6.40E-06

Fig. 5. Pancreas genes are downregulated with ectopic expression of FOXA1 and liver genes in *Grg3/4* mutants. (A) Volcano plot showing differentially expressed genes in e18.5 pancreata from *Pdx1:Cre* controls versus *Pdx1:Cre; Grg3/4* mutants using DESeq2 analysis. Downregulated genes are indicated by magenta dots and upregulated genes are indicated by green dots. White dots represent predicted *Foxa1* target genes that are differentially expressed in the dataset. *P*adj cutoff=0.05. *n*=3 for each genotype. (B) Gene ontology (GO) term analysis of up- and downregulated genes. Asterisks indicate pathways associated with liver metabolism. (C) Select list of downregulated genes related to pancreas development and hormone expression. (D) Top 10 upregulated genes sorted by fold change. (E) Immunofluorescence staining of e12.5 pancreata showing overlap of PDX1 and FOXA1 protein in *Pdx1:Cre; Grg3/4* mutants. Scale bars: 50 µm. (F) Validation of the upregulated liver gene *Serpina1e* using RNAscope in e16.5 *Pdx1:Cre; Grg3/4* pancreas. Scale bars: 50 µm. (G) Immunofluorescence staining in e16.5 mice of alpha1 antitrypsin (AAT, encoded by *Serpina1a-e* genes) shows that upregulation of mRNA does not correlate with protein expression levels. White arrowheads indicate AAT cells in *Pdx1:Cre; Grg3/4* pancreas. Scale bars: 50 µm.

have a significant reduction in β cell number perinatally, and β cell-specific loss of *Neurod1* results in the failure of β cell expansion by proliferation (Naya et al., 1997; Gu et al., 2010; Mastracci et al., 2013a; Romer et al., 2019). To determine whether *Pdx1:Cre; Grg3/4* mutants phenocopy *Neurod1*$^{-/-}$ mice, we assessed β cell proliferation and apoptosis. In both e16.5 and P2 pancreata, the percentage of proliferating Ki67^{+} β cells was significantly decreased in *Pdx1:Cre; Grg3/4* mutants compared with control pancreata (Fig. 6C,D), whereas, by TUNEL staining, we observed no β cell apoptosis in either control or mutant pancreata (data not shown). These findings suggest that the decrease in β cells in the *Pdx1:Cre; Grg3/4* mutants was primarily due to defects in β cell proliferation, consistent with previously described *Neurod1* mutant phenotypes (Romer et al., 2019).

Development (2021) 148, dev192401. doi:10.1242/dev.192401

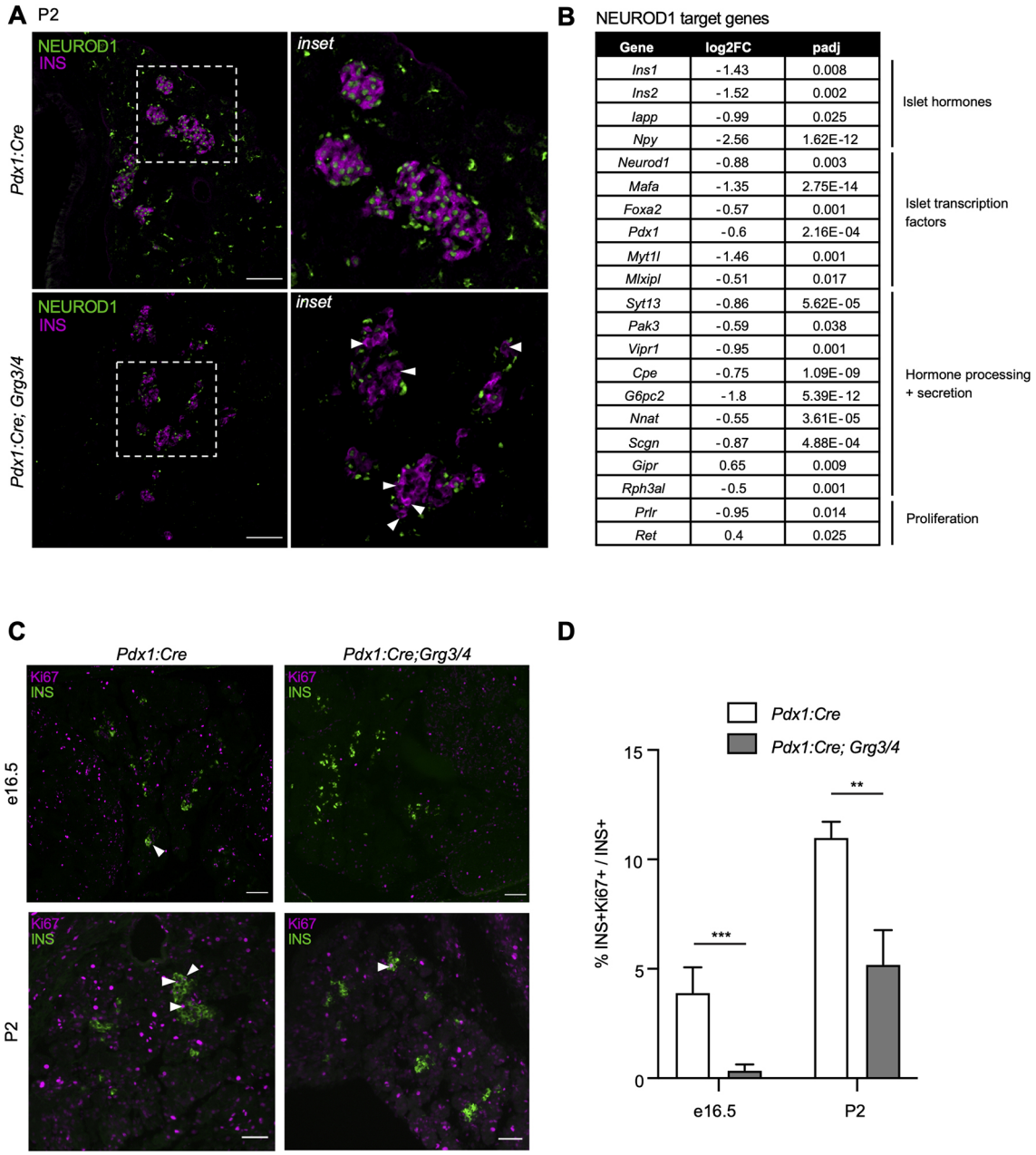

Fig. 6. *Grg3/4* mutants have a loss of NEUROD1, target gene expression, and proliferation of β cells. (A) Immunofluorescence staining for INS and NEUROD1 in P2 pancreata. White arrowheads indicate INS$^+$ β cells without NEUROD1. INS$^-$/NEUROD1$^+$ cells likely represent non-β endocrine cells. Right-hand panels are magnifications of the boxed areas on the left. Scale bars: 100 µm. (B) List of differentially expressed *Neurod1* target genes in e18.5 pancreata. (C) Immunofluorescence analysis of proliferating β cells using the proliferative marker Ki67 in e16.5 and P2 mice. White arrowheads indicate INS$^+$Ki67$^+$ cells. Scale bars: 50 µm. (D) Percentage of Ki67$^+$ cells in INS$^+$ cells as shown in C. *n*=3-6 for each genotype. $^{**}P\leq0.01$; $^{***}P\leq0.001$; two-tailed Student's *t*-test.

DISCUSSION

The transcription factor networks controlling pancreas development and function have been extensively characterized. Although it is known that many of these transcription factors rely on interactions with co-factors to allow cell-specific gene expression, only a small number of studies have explored their respective functions *in vivo* (McKenna et al., 2015; Spaeth et al., 2016, 2019; Yang et al., 2020). The *Groucho* family of co-repressors has been documented in many developmental systems to play integral roles in promoting cell fate decisions via transcriptional repression (Agarwal et al., 2015). In the present study, we used phenotypic and transcriptomic analyses to characterize GRG function in the developing murine pancreas. We found that pancreas-specific loss of *Grg3* resulted in ectopic expression of *Grg4* as a compensatory mechanism preventing a more severe phenotype in *Grg3* single mutant animals. When both *Grg3* and *Grg4* were deleted from pancreatic progenitors, the hepatic transcription factor FOXA1 is no longer repressed in the pancreas lineage, resulting in ectopic expression of liver genes in embryonic pancreata (Fig. 7). We further show that β cells from *Pdx1:Cre; Grg3/4* mutants lack NEUROD1 and fail to proliferate normally (Fig. 7). Together, these results uncover novel gene regulatory roles of GRGs in pancreas development and improve our understanding of co-factor-mediated transcriptional repression.

Development (2021) 148, dev192401. doi:10.1242/dev.192401

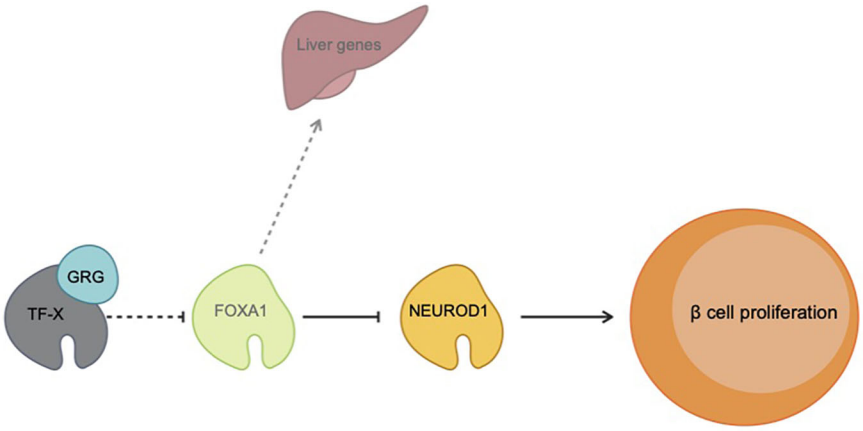

Fig. 7. Model of GRG function in pancreas development. During normal pancreas development, GRG3/4 interacts with transcription factors (TF-X) to either directly or indirectly repress the master liver regulator *Foxa1* in the pancreas lineage. Loss of GRG3/4-mediated repression results in ectopic FOXA1 protein, which both erroneously activates the liver program in the pancreas and represses expression of the β cell transcription factor gene *Neurod1*. Decreased NEUROD1 levels in β cells leads to a loss of β proliferation, early lethality, and hyperglycemia.

Until recently, there have been very few studies exploring the role of transcriptional repression in pancreas development. Two prior publications that explored GRG-mediated repression in the pancreas were limited by the early embryonic lethality of the *Grg3* null mice (Metzger et al., 2012, 2014). These studies provided evidence of the importance of *Grg3* the pancreas, but lacked the precision afforded by the pancreas-specific deletion of *Grg3* using a *Cre-Lox* system. Although the use of cultured e12.5 pancreatic bud explants from $Grg3^{-/-}$ embryos allowed the investigators to assess later stages of pancreas development, the caveats associated with ectopic explant techniques may have affected their data interpretation, as we were not able to replicate their findings that endocrine cells failed to delaminate from the trunk epithelium due to a loss of E-cadherin repression, resulting in severe endocrine differentiation defects (Metzger et al., 2012). It is also possible that their pancreatic phenotypes were affected by pancreas non-autonomous defects as $Grg3^{-/-}$ embryos are significantly smaller and have defects in many different tissues that could have indirect effects on pancreas development (Gasperowicz et al., 2013).

Previous work from our lab demonstrated that the GRG3-interacting domain of NKX2-2 ($Nkx2.2^{TN}$) is required to repress the α cell master regulator *Arx* in β cells. Loss of this interaction resulted in demethylation of the *Arx* promoter, significant β-to-α reprogramming, and lethality due to severe hyperglycemia (Papizan et al., 2011). Interestingly, perturbing this interaction by removing GRG3/4 from the pancreas did not phenocopy the $Nkx2.2^{TN}$ mutation – we did not observe upregulation of *Arx* nor an increase in α cells embryonically or postnatally. This suggests that the NKX2-2 TN domain has additional functions beyond its interaction with GRGs or that GRG-mediated repression during pancreas development extends beyond interactions with NKX2-2 to counteract the $Nkx2.2^{TN}$ phenotype. It was also surprising that deletion of *Grg3* and combined deletion of *Grg3/4* did not display a more severe phenotype. NKX6-1, another essential β cell transcription factor that results in a >90% reduction of β cells when deleted (Sander et al., 2000; Henseleit et al., 2005; Taylor et al., 2013), interacts with GRG4 in the central nervous system and promotes proper neural tube patterning (Muhr et al., 2001). Therefore, NKX6-1 would be expected to at least partially rely on GRG interactions in the pancreas to exert its function. Additional pancreas transcription factors that contain GRG interaction domains are PAX4/6, FOXA1/2, HES1, SOX9 and ARX (Buscarlet and Stifani, 2007; Jennings and Ish-Horowicz, 2008; Agarwal et al., 2015). Although these candidates have not yet been confirmed to interact with GRGs in the pancreas, we expected that loss of GRG function in the pancreas would produce an extremely severe phenotype that at least partially reflected the combined phenotypes of these essential pancreatic transcriptional regulators. Because mice deleted for *Grg3/Grg4* in the pancreas do not phenocopy mutations in interacting transcription factors, either these essential pancreatic transcriptional regulators do not rely on GRG interactions to exert their functions or there is inherent redundancy in the system to compensate for the absence of GRG functions. This redundancy would likely operate through non-GRG dependent pathways as GRG2 deletion had no effect on pancreas development, either alone or in combination with deletion of *Grg3*, and GRG1 expression could not be detected in embryonic pancreas of either wild-type or any of the Grg mutant animals.

One novel phenotype we did discover in the *Pdx1:Cre; Grg3/4* mutants was that FOXA1, a master regulator of the hepatic program, was no longer repressed in the pancreas throughout development and postnatally. Previous studies have suggested that FOXA1 acts redundantly in FOXA2-deficient pancreata; however, recent single-cell RNA-seq data suggest that *Foxa1* is expressed at extremely low to undetectable levels in the developing pancreas (Krentz et al., 2018) and loss of FOXA1 alone does not affect pancreas function (Gao et al., 2010). Overexpression of *Foxa1* in the pancreas has not been previously reported and the direct consequences on gene expression were difficult to dissect given the large number of dysregulated genes in *Pdx1:Cre; Grg3/4* mutants. Interestingly, a number of liver genes were also ectopically expressed in the pancreas, which is consistent with previous studies that demonstrated that *Grg3* expression was necessary to suppress the liver program in the developing foregut endoderm (Santisteban et al., 2010). However, we were unable to detect upregulation of the corresponding liver proteins. As the general translational machinery should be intact in the mutant islets, the disconnect between RNA and protein expression could reflect the absence of liver-specific proteins that would be needed to stabilize and/or facilitate the translation of these cell-specific transcripts. With the advent of single-cell genomic and proteomic technologies, there is a growing appreciation for a disconnect between mRNA and protein levels in several cellular contexts (Liu et al., 2016). Future studies that explore tissue-specific translational control could provide important information on novel mechanisms that regulate pancreas versus liver lineage programs.

Because the consensus sequence and targets of FOXA1 have been identified in other biological contexts, we were able to predict additional genes that were differentially regulated by FOXA1 in this system. From these analyses, we identified *Neurod1* as a potential FOXA1 target that was significantly downregulated in *Pdx1:Cre; Grg3/4* mutants. The phenotype identified here is strikingly similar

Development (2021) 148, dev192401. doi:10.1242/dev.192401

to that of *Neurod1*$^{-/-}$ mice: reduced β cell proliferation resulting in failed expansion of the β cell population, leading to severe hyperglycemia and early lethality (Naya et al., 1997; Itkin-Ansari et al., 2005; Mastracci et al., 2013a; Romer et al., 2019). Although we can attribute much of the pancreas phenotype of *Pdx1:Cre; Grg3/4* mutant mice to the dysregulation of *Foxa1* and *Neurod1*, there were almost 2000 genes perturbed in mutant pancreata, suggesting that additional pathways are upregulated when GRG function is disrupted. These results provide strong evidence for the necessity of GRG-mediated transcriptional repression, both direct and indirect, in pancreas development. Future studies will focus on identification of the full cohort of GRG-interacting factors in the pancreas, the genes that are regulated by these complexes, and molecular mechanism underlying GRG-mediated gene repression in this system.

Transcriptional repression during organogenesis is widely recognized as a crucial component of proper tissue development (Gary and Levin, 1996; Meehan, 2003; Golson and Kaestner, 2017; Jambhekar et al., 2019). Loss of repression leads to aberrant gene expression and perturbations in cell-specific genetic programs. Although many studies have previously focused on the mechanisms activating tissue-specific gene expression, our understanding of the factors involved in inducing and maintaining repression of other genetic programs is still evolving. Ultimately, further insight into the mechanisms that promote cell- and tissue-specific gene programs while concurrently repressing other cell and tissue identities could enable us to improve therapeutic options for diabetic patients.

MATERIALS AND METHODS

Animal models and maintenance

Animals were maintained under protocol 00045 as approved by the University of Colorado Denver Institutional Animal Care and Use Committee (IACUC). All mice were maintained on a mixed C57BL6 genetic background. Animals were group-housed by sex with up to five siblings per cage with *ad libitum* food and water. Cages were held at 22°C, changed once every 2 weeks, and regularly monitored for virus and parasite infection. Euthanasia was performed by CO_2 inhalation with cervical dislocation as a secondary method following asphyxiation. For timed pregnancies, presence of a vaginal plug in the morning was defined as e0.5. All mice and embryos were genotyped with primers listed in Table S2 using PCR with GoTaq DNA Polymerase Mastermix (Promega). The generation of *Pdx1:Cre, Grg3*^{flox}, and *Grg4*^{flox} mice have been previously described (Hingorani et al. Tuveson, 2003; Villanueva et al., 2011; Wheat et al., 2014). *Pdx1:Cre* mice are available at Jackson Laboratories: B6.FVB-Tg(Pdx1-cre)6Tuv/J (cat. #RRID:IMSR_JAX:014647).

Generation of *Grg2* mice

We obtained *Grg2/TLE2* knockout embryonic stem cells (*Grg2/*Tle2$^{tm1(KOMP)Vlcg}$) through the Mouse Mouse Resource and Research Center (RRID:MMRRC_050067-UCD; http://velocigene.com/komp/detail/12600). The *Grg2* null embryonic stem cells were injected into the blastocysts of F1 hybrid (C57BL/6×129) mice at the Columbia University Transgenic core to generate three independent lines of mice carrying a null mutation that eliminated *Grg2* expression. The mice were genotyped using primers for the *Grg2* wild-type alleles oRS31 (TLE2WT-R): 5′-GGGATTCTAGGATTC-TAGGCAGGGC-5′ and oRS32 (TLE2WT-F): 3′-TTGAGGCATGGTCT-TGCTTTGTAGC-3′; and the mutant alleles oRS28 (NeoF): 5′-GCAGC-CTCTGTTCCACATACACTTCA-3′ and oRS30 (TLE2-R): 5′-AGAGCC-AGGAAGATGGTTCAGTTGG-3′. These mice were subsequently bred and maintained on a C57BL6 genetic background. Complete deletion of *Grg2* was verified by qRT-PCR (Fig. 1D).

RNA *in situ* hybridization

All GRG probes were generated from full-length cDNAs. Sense and antisense probes were labeled with the DIG RNA labeling mix (Roche Applied Science). RNA *in situ* hybridization was performed as previously described (Mastracci et al., 2013b).

Blood glucose

Ad libitum blood glucose measurements were taken using tail vein blood samples. Glucose concentrations were determined using a Contour 7151H glucose meter with Contour 7097C test strips.

Glucose tolerance tests

Mice were fasted overnight for 12 h followed by an intraperitoneal injection with glucose (2 mg/g body weight). Tail vein blood samples were collected at 0, 15, 30, 60 and 120 min after injection. Glucose concentrations were determined using a Contour 7151H glucose meter with Contour 7097C test strips.

Insulin content

Islets (20 per well) were cultured in Kreb's buffer with a glucose concentration of 2.8 mM for 1 h in a 12-well plate. Islets were then disrupted using a homogenizer in 50 µl of lysis buffer (150 mM NaCl, 50 mM Tris-HCl pH 8.0, 1% IGEPAL) and cellular insulin content was extracted by acid ethanol and measured by ultrasensitive insulin ELISA (CrystalChem).

Tissue preparation and immunofluorescence

Timed pregnant females were sacrificed and embryos were removed and placed directly into ice-cold PBS (pH 7.4). For e12.5-e16.5 embryos, heads were removed and remaining embryos were placed in 4% paraformaldehyde (PFA) for 4 h at 4°C. For P2 animals, abdominal organs were dissected and placed in 4% PFA for 4 h at 4°C. Adult whole pancreata were dissected and placed in 4% PFA for 4 h at 4°C. Tissue was cryo-preserved in 30% sucrose-PBS solution for overnight at 4°C followed by embedding and freezing in Optimum Cutting Temperature (O.C.T.) on dry ice. Tissue was stored at −80°C until 10 µm cryo-sections were collected for analyses using a Microm HM 525 cryostat.

For immunofluorescence analysis, sections were washed in PBS and 0.01% Triton X-100 (PBS-T) and blocked with 2% normal donkey serum (NDS) for 30 min at room temperature (RT). Primary antibodies were diluted in 2% NDS and incubated on sections overnight at 4°C in a humidified chamber. Sections were washed with PBS-T and incubated for 2-3 h at RT with secondary antibodies diluted in 2% NDS. Sections were washed with PBS-T and incubated with DAPI (Fisher Scientific, D1306) diluted 1:1000 in PBS-T for 15 min at RT. Sections were washed with PBS-T and mounted with VECTASHIELD Hardset Antifade Mounting Medium (Vector Laboratories, H-1400). All primary and secondary antibodies can be found in Table S3.

High-magnification images, including all images showing bihormonal cells, were taken using a Zeiss Confocal LSM800 microscope and processed with Zen, ImageJ and Adobe Photoshop software. Lower magnification images for quantification purposes were taken using a Leica DM5500B microscope.

RNAscope

RNAscope was performed as described in ACD Biosciences RNAscope Fluorescent Multiplex Kit Quick Guide (https://acdbio.com/documents/product-documents). Samples were fixed and sectioned as described above. The samples were then post-fixed at 4°C overnight in 4% PFA, followed by dehydration by ethanol and drying. Slides were treated with hydrogen peroxide for and antigen retrieval by boiling in Target Retrieval. Slides were washed with deionised (DI) water and subjected to mild protease digestion (Protease III) for 20 min in a humified chamber, washed again in DI water and incubated with probes purchased from ACD Biosciences [RNAscope Probe-Mm-*Ins2*-C1 (414661), -*Serpina1e*-C2 (88277)] for 2 h at 40°C. Slides were washed with Wash Buffer and placed in 5× SSC overnight. Slides were again washed and incubated in AMP1, -2 and -3 solutions for 30 min, 30 min,and 15 min, respectively, at 40°C, with washes in between each incubation. To develop signal, we used Opal Dyes 570 and 620 (RNAscope Multiplex Fluorescent Detection Kit v2) diluted in Multiplex

Development (2021) 148, dev192401. doi:10.1242/dev.192401

TSA buffer. Each channel was developed sequentially by incubating samples in HRP-C1/2 for 15 min at 40°C, washed, and then incubated in the pre-diluted Opal Dye for 30 min at 40°C. Slides were then washed and incubated in HRP Blocker for 15 min at 40°C. This solution was removed, and slides were again washed followed by a 10 min incubation at RT with DAPI. Slides were mounted using Prolong Gold Mounting Media (Invitrogen) and imaged at 40× on a Zeiss LSM800 confocal microscope.

Morphometric analysis

Quantification of hormone and pancreas area was performed using ImageJ software and thresholding of individual color channels. Pancreas area was outlined and DAPI$^+$ pixels were quantified. Hormone area was calculated as the hormone$^+$ area divided by the DAPI$^+$ area. For Ki67 quantification, all insulin$^+$ β cells and Ki67/insulin double-positive cells were counted and percentage proliferation was calculated by dividing Ki67/insulin$^+$ cell counts by total insulin$^+$ cell counts. A total of five slides and ten slides, evenly spaced throughout the entire pancreas, were quantified per sample for e16.5 and P2 time points, respectively.

RNA extraction and RT-qPCR

Whole pancreata were collected from embryos and flash frozen in Buffer RLT (Qiagen). Total RNA extractions were performed using the RNeasy Mini Kit (Qiagen) and eluted in 30 µl RNase-free water. cDNA was generated with 500 ng of RNA as template using the iScript cDNA Synthesis Kit (Bio-Rad). The resulting cDNA was diluted to 1 ng/µl and 4 µl were used in each qPCR reaction using the SsoAdvanced Universal Probes Supermix (Bio-Rad) with Taqman probes (Table S4). Reactions were run on the Bio-Rad CFX96 Real Time PCR Detection System. Expression levels were normalized to cyclophilin B (also known as peptidylprolyl isomerase B) or *Actb* and quantified using the $2^{-\Delta\Delta CT}$. Control samples were set to one for each gene to determine expression changes in mutants.

RNA sequencing

RNA was extracted as described and RNA integrity number (RIN) was determined using the Eukaryote Total RNA Nano Kit for the Agilent 2100 Bioanalyzer. Libraries were prepared from samples with RIN values >8.0 using the Universal Plus mRNA-Seq with NuQuant kit (NuGen), then subjected to high-throughput RNA sequencing using the NovaSEQ 6000 for paired end sequencing (2×150) from PolyA selected total RNA by the University of Colorado Cancer Center Genomics and Microarray Core. Reads were quality checked using fastQC and adapters trimmed using trim-galore (http://www.bioinformatics.babraham.ac.uk/projects/trim_galore/). Reads were aligned to the mm10 genome using HISAT2 and mapped to genes using HTSeq with the Ensemble genome: Mus_musculus.GRCm38.95.gtf (Anders et al., 2015; Kim et al., 2015). Differential gene expression was determined using DESeq2 in R (Love et al., 2014). Gene ontology enrichment analysis was performed using Panther (http://pantherdb.org/). Differentially expressed *Foxa1* known and predicted target genes were assessed using Harmonizome with the TRANSFAC Curated Transcription Factor Targets database (http://amp.pharm.mssm.edu/Harmonizome/).

Western blotting

Nuclear protein lysates were prepared from excised P0 pancreata using the Nuclear Extract Kit (Active Motif). Approximately 20 µg of each sample was loaded onto a 10% Bis-Tris polyacrylamide gel (Invitrogen). Proteins were transferred to PVDF membrane and the membrane blocked in 5% milk for 30 min, incubated with rabbit anti-TLE3 (1:100, sc-9124, Santa Cruz Biotechnology) and rabbit anti-GAPDH (1:1000, ab9485, Abcam) overnight at 4°C, washed, incubated with anti-rabbit-HRP (1:10,000, 32260, Zymed) for 1 h at RT, washed, and developed with the Western Lightning chemiluminescence kit (GE Biosciences).

Quantification and statistical analysis

Graphs and statistical analyses were generated using GraphPad Prism 8. All values are shown as mean±s.d. *P*-values were calculated using two-tailed Student's *t*-test. Each *n* represents an individual animal and *n* values for all experiments are listed in the figure legends. For the RNA-sequencing experiments, *P*adjusted ≤0.05 was used as the cutoff for differentially expressed genes (defined by the Benjamini–Hochberg procedure for multiple hypothesis testing).

Acknowledgements

We thank members of the Sussel lab for helpful feedback on this project and especially Michelle Guney, Nicole Moss and David Lorberbaum for critical reading of the manuscript. We also thank Dr Peter Tontonoz (University of California Los Angeles) and Dr David Sweetser (Massachusetts General Hospital) for generously providing us with the *Grg3 and Grg4 floxed* mice, respectively. We are grateful for technical assistance for many specialized techniques and analyses presented here: RNA sequencing was conducted by the University of Colorado Denver Microarray and Genomics core and advice to A.T. for the RNA sequencing computational analysis was provided by the CU Denver RNA Biosciences Initiative.

Competing interests

The authors declare no competing or financial interests.

Author contributions

Conceptualization: A.T., R.A.S., L.S.; Methodology: A.T., R.A.S., L.S.; Validation: A.T.; Formal analysis: A.T., R.A.S., D.G., A.P., A.N., L.S.; Investigation: A.T., R.A.S., D.G., A.P., A.N., L.S.; Resources: L.S.; Data curation: A.T.; Writing - original draft: A.T.; Writing - review & editing: A.T., R.A.S., L.S.; Supervision: L.S.; Project administration: L.S.; Funding acquisition: L.S.

Funding

Support for the project was provided by the National Institute of Diabetes and Digestive and Kidney Diseases (R01 DK082590 and P30 DK116073 to L.S., F31 DK122634 to A.T., F31 DK107028 to R.A.S.). Deposited in PMC for release after 12 months.

Data availability

Raw RNA-seq fastq files have been deposited in Gene Expression Omnibus under accession numbers GSE149889 (e15.5 sorted NEUROG3-EGFP cells) and GSE149891 (e18.*5 Pdx1:Cre; Grg3* and *Pdx1:Cre; Grg3/4* pancreata).

Supplementary information

Supplementary information available online at
https://dev.biologists.org/lookup/doi/10.1242/dev.192401.supplemental

Peer review history

The peer review history is available online at
https://dev.biologists.org/lookup/doi/10.1242/dev.192401.reviewer-comments.pdf

References

Agarwal, M., Kumar, P. and Mathew, S. J. (2015). The Groucho/Transducin-like enhancer of split protein family in animal development. *IUBMB Life* **67**, 472-481. doi:10.1002/iub.1395

American Diabetes Association. (2020). 2. Classification and diagnosis of diabetes: standards of medical care in diabetes-2020. *Diabetes Care* **43**, S14-S31. doi:10.2337/dc20-S002

Anders, S., Pyl, P. T. and Huber, W. (2015). HTSeq–a Python framework to work with high-throughput sequencing data. *Bioinformatics* **31**, 166-169. doi:10.1093/bioinformatics/btu638

Ang, S. L., Wierda, A., Wong, D., Stevens, K. A., Cascio, S., Rossant, J. and Zaret, K. S. (1993). The formation and maintenance of the definitive endoderm lineage in the mouse: involvement of HNF3/forkhead proteins. *Development* **119**, 1301-1315.

Buscarlet, M. and Stifani, S. (2007). The 'Marx' of Groucho on development and disease. *Trends Cell Biol.* **17**, 353-361. doi:10.1016/j.tcb.2007.07.002

Cai, Y., Brophy, P. D., Levitan, I., Stifani, S. and Dressler, G. R. (2003). Groucho suppresses Pax2 transactivation by inhibition of JNK-mediated phosphorylation. *EMBO J.* **22**, 5522-5529. doi:10.1093/emboj/cdg536

Cernea, S. and Dobreanu, M. (2013). Diabetes and beta cell function: from mechanisms to evaluation and clinical implications. *Biochem. Med.* **23**, 266-280. doi:10.11613/BM.2013.033

Chao, C. S., Loomis, Z. L., Lee, J. E. and Sussel, L. (2007). Genetic identification of a novel NeuroD1 function in the early differentiation of islet α, PP and ε cells. *Dev. Biol.* **312**, 523-532. doi:10.1016/j.ydbio.2007.09.057

Chen, G., Fernandez, J., Mische, S. and Courey, A. J. (1999). A functional interaction between the histone deacetylase Rpd3 and the corepressor groucho in *Drosophila* development. *Genes Dev.* **13**, 2218-2230. doi:10.1101/gad.13.17.2218

Collombat, P., Mansouri, A., Hecksher-Sørensen, J., Serup, P., Krull, J., Gradwohl, G. and Gruss, P. (2003). Opposing actions of Arx and Pax4 in endocrine pancreas development. *Genes Dev.* **17**, 2591-2603. doi:10.1101/gad.269003

Collombat, P., Hecksher-Sorensen, J., Broccoli, V., Krull, J., Ponte, I., Mundiger, T., Smith, J., Gruss, P., Serup, P. and Mansouri, A. (2005). The simultaneous loss of Arx and Pax4 genes promotes a somatostatin-producing cell fate specification at the expense of the α- and β-cell lineages in the mouse endocrine pancreas. *Development* **132**, 2969-2980. doi:10.1242/dev.01870

Dassaye, R., Naidoo, S. and Cerf, M. E. (2016). Transcription factor regulation of pancreatic organogenesis, differentiation and maturation. *Islets* **8**, 13-34. doi:10.1080/19382014.2015.1075687

Eberhard, D., Jiménez, G., Heavey, B. and Busslinger, M. (2000). Transcriptional repression by Pax5 (BSAP) through interaction with corepressors of the Groucho family. *EMBO J.* **19**, 2292-2303. doi:10.1093/emboj/19.10.2292

Gao, N., LeLay, J., Vatamaniuk, M. Z., Rieck, S., Friedman, J. R. and Kaestner, K. H. (2008). Dynamic regulation of Pdx1 enhancers by Foxa1 and Foxa2 is essential for pancreas development. *Genes Dev.* **22**, 3435-3448. doi:10.1101/gad.1752608

Gao, N., Le Lay, J., Qin, W., Doliba, N., Schug, J., Fox, A. J., Smirnova, O., Matschinsky, F. M. and Kaestner, K. H. (2010). Foxa1 and Foxa2 maintain the metabolic and secretory features of the mature β-cell. *Mol. Endocrinol.* **24**, 1594-1604. doi:10.1210/me.2009-0513

Gary, S. and Levin, M. (1996). Transcriptional repression in development. *Curr. Opin. Cell Biol.* **8**, 358-364. doi:10.1016/S0955-0674(96)80010-X

Gasperowicz, M., Surmann-Schmitt, C., Hamada, Y., Otto, F. and Cross, J. C. (2013). The transcriptional co-repressor TLE3 regulates development of trophoblast giant cells lining maternal blood spaces in the mouse placenta. *Dev. Biol.* **382**, 1-14. doi:10.1016/j.ydbio.2013.08.005

Golson, M. L. and Kaestner, K. H. (2017). Epigenetics in formation, function, and failure of the endocrine pancreas. *Mol. Metab.* **6**, 1066-1076. doi:10.1016/j.molmet.2017.05.015

Gu, C., Stein, G. H., Pan, N., Goebbels, S., Hörnberg, H., Nave, K.-A., Herrera, P., White, P., Kaestner, K. H., Sussel, L. et al. (2010). Pancreatic β cells require NeuroD to achieve and maintain functional maturity. *Cell Metab.* **11**, 298-310. doi:10.1016/j.cmet.2010.03.006

Gutiérrez, G. D., Bender, A. S., Cirulli, V., Mastracci, T. L., Kelly, S. M., Tsirigos, A., Kaestner, K. H. and Sussel, L. (2017). Pancreatic β cell identity requires continual repression of non-β cell programs. *J. Clin. Investig.* **127**, 244-259. doi:10.1172/JCI88017

Henseleit, K. D., Nelson, S. B., Kuhlbrodt, K., Hennings, J. C., Ericson, J. and Sander, M. (2005). NKX6 transcription factor activity is required for α- and β-cell development in the pancreas. *Development* **132**, 3139-3149. doi:10.1242/dev.01875

Hingorani, S. R., Petricoin, E. F., Maitra, A., Rajapakse, V., King, C., Jacobetz, M. A., Ross, S., Conrads, T. P., Veenstra, T. D., Hitt, B. A. et al. (2003). Preinvasive and invasive ductal pancreatic cancer and its early detection in the mouse. *Cancer Cell* **4**, 437-450. doi:10.1016/S1535-6108(03)00309-X

Hoffman, B. G., Zavaglia, B., Beach, M. and Helgason, C. D. (2008). Expression of Groucho/TLE proteins during pancreas development. *BMC Dev. Biol.* **8**, 81. doi:10.1186/1471-213X-8-81

Itkin-Ansari, P., Marcora, E., Geron, I., Tyrberg, B., Demeterco, C., Hao, E., Padilla, C., Ratineau, C., Leiter, A., Lee, J. E. et al. (2005). NeuroD1 in the endocrine pancreas: localization and dual function as an activator and repressor. *Dev. Dyn.* **233**, 946-953. doi:10.1002/dvdy.20443

Iype, T., Taylor, D. G., Ziesmann, S. M., Garmey, J. C., Watada, H. and Mirmira, R. G. (2004). The transcriptional repressor Nkx6.1 also functions as a deoxyribonucleic acid context-dependent transcriptional activator during pancreatic β-cell differentiation: evidence for feedback activation of the nkx6.1 gene by Nkx6.1. *Mol. Endocrinol.* **18**, 1363-1375. doi:10.1210/me.2004-0006

Jambhekar, A., Dhall, A. and Shi, Y. (2019). Roles and regulation of histone methylation in animal development. *Nat. Rev. Mol. Cell Biol.* **20**, 625-641. doi:10.1038/s41580-019-0151-1

Jangal, M., Couture, J.-P., Bianco, S., Magnani, L., Mohammed, H. and Gévry, N. (2014). The transcriptional co-repressor TLE3 suppresses basal signaling on a subset of estrogen receptor α target genes. *Nucleic Acids Res.* **42**, 11339-11348. doi:10.1093/nar/gku791

Jennings, B. H. and Ish-Horowicz, D. (2008). The Groucho/TLE/Grg family of transcriptional co-repressors. *Genome Biol.* **9**, 205. doi:10.1186/gb-2008-9-1-205

Jensen, J., Pedersen, E. E., Galante, P., Hald, J., Heller, R. S., Ishibashi, M., Kageyama, R., Guillemot, F., Serup, P. and Madsen, O. D. (2000). Control of endodermal endocrine development by Hes-1. *Nat. Genet.* **24**, 36-44. doi:10.1038/71657

Jørgensen, M. C., Ahnfelt-Rønne, J., Hald, J., Madsen, O. D., Serup, P. and Hecksher-Sørensen, J. (2007). An illustrated review of early pancreas development in the mouse. *Endocr. Rev.* **28**, 685-705. doi:10.1210/er.2007-0016

Kaestner, K. H. (2010). The FoxA factors in organogenesis and differentiation. *Curr. Opin. Genet. Dev.* **20**, 527-532. doi:10.1016/j.gde.2010.06.005

Kim, D., Langmead, B. and Salzberg, S. L. (2015). HISAT: a fast spliced aligner with low memory requirements. *Nat. Methods* **12**, 357-360. doi:10.1038/nmeth.3317

Krentz, N. A. J., Lee, M. Y. Y., Xu, E. E., Sproul, S. L. J., Maslova, A., Sasaki, S. and Lynn, F. C. (2018). Single-cell transcriptome profiling of mouse and hESC-derived pancreatic progenitors. *Stem Cell Rep.* **11**, 1551-1564. doi:10.1016/j.stemcr.2018.11.008

Lee, C. S., Friedman, J. R., Fulmer, J. T. and Kaestner, K. H. (2005). The initiation of liver development is dependent on Foxa transcription factors. *Nature* **435**, 944-947. doi:10.1038/nature03649

Li, L.-C., Qiu, W.-L., Zhang, Y.-W., Xu, Z.-R., Xiao, Y.-N., Hou, C., Lamaoqiezhong, Yu, P., Cheng, X. and Xu, C.-R. (2018). Single-cell transcriptomic analyses reveal distinct dorsal/ventral pancreatic programs. *EMBO Rep.* **19**, e46148. doi:10.15252/embr.201846148

Linderson, Y., Eberhard, D., Malin, S., Johansson, A., Busslinger, M. and Pettersson, S. (2004). Corecruitment of the Grg4 repressor by PU.1 is critical for Pax5-mediated repression of B-cell-specific genes. *EMBO Rep.* **5**, 291-296. doi:10.1038/sj.embor.7400089

Liu, Y., Beyer, A. and Aebersold, R. (2016). On the dependency of cellular protein levels on mRNA abundance. *Cell* **165**, 535-550. doi:10.1016/j.cell.2016.03.014

Love, M. I., Huber, W. and Anders, S. (2014). Moderated estimation of fold change and dispersion for RNA-seq data with DESeq2. *Genome Biol.* **15**, 550. doi:10.1186/s13059-014-0550-8

Marçal, N., Patel, H., Dong, Z., Belanger-Jasmin, S., Hoffman, B., Helgason, C. D., Dang, J. and Stifani, S. (2005). Antagonistic effects of Grg6 and Groucho/TLE on the transcription repression activity of brain factor 1/FoxG1 and cortical neuron differentiation. *Mol. Cell. Biol.* **25**, 10916-10929. doi:10.1128/MCB.25.24.10916-10929.2005

Mastracci, T. L., Anderson, K. R., Papizan, J. B. and Sussel, L. (2013a). Regulation of Neurod1 contributes to the lineage potential of Neurogenin3+ endocrine precursor cells in the pancreas. *PLoS Genet.* **9**, e1003278. doi:10.1371/journal.pgen.1003278

Mastracci, T. L., Lin, C.-S. and Sussel, L. (2013b). Generation of mice encoding a conditional allele of Nkx2.2. *Transgenic Res.* **22**, 965-972. doi:10.1007/s11248-013-9700-0

McKenna, B., Guo, M., Reynolds, A., Hara, M. and Stein, R. (2015). Dynamic recruitment of functionally distinct Swi/Snf chromatin remodeling complexes modulates Pdx1 activity in islet β cells. *Cell Rep.* **10**, 2032-2042. doi:10.1016/j.celrep.2015.02.054

Meehan, R. R. (2003). DNA methylation in animal development. *Semin. Cell Dev. Biol.* 14, 53-65. doi:10.1016/S1084-9521(02)00137-4

Metzger, D. E., Gasperowicz, M., Otto, F., Cross, J. C., Gradwohl, G. and Zaret, K. S. (2012). The transcriptional co-repressor Grg3/Tle3 promotes pancreatic endocrine progenitor delamination and β-cell differentiation. *Development* **139**, 1447-1456. doi:10.1242/dev.072892

Metzger, D. E., Liu, C., Ziaie, A. S., Naji, A. and Zaret, K. S. (2014). Grg3/TLE3 and Grg1/TLE1 induce monohormonal pancreatic β-cells while repressing α-cell functions. *Diabetes* **63**, 1804-1816. doi:10.2337/db13-0867

Milili, M., Gauthier, L., Veran, J., Mattei, M.-G. and Schiff, C. (2002). A new Groucho TLE4 protein may regulate the repressive activity of Pax5 in human B lymphocytes. *Immunology* **106**, 447-455. doi:10.1046/j.1365-2567.2002.01456.x

Monaghan, A. P., Kaestner, K. H., Grau, E. and Schutz, G. (1993). Postimplantation expression patterns indicate a role for the mouse forkhead/HNF-3 alpha, beta and gamma genes in determination of the definitive endoderm, chordamesoderm and neuroectoderm. *Development* **119**, 567-578.

Muhr, J., Andersson, E., Persson, M., Jessell, T. M. and Ericson, J. (2001). Groucho-mediated transcriptional repression establishes progenitor cell pattern and neuronal fate in the ventral neural tube. *Cell* **104**, 861-873. doi:10.1016/S0092-8674(01)00283-5

Naya, F. J., Huang, H.-P., Qiu, Y., Mutoh, H., DeMayo, F. J., Leiter, A. B. and Tsai, M.-J. (1997). Diabetes, defective pancreatic morphogenesis, and abnormal enteroendocrine differentiation in BETA2/neuroD-deficient mice. *Genes Dev.* **11**, 2323-2334. doi:10.1101/gad.11.18.2323

Pan, F. C. and Wright, C. (2011). Pancreas organogenesis: from bud to plexus to gland. *Dev. Dyn.* **240**, 530-565. doi:10.1002/dvdy.22584

Papizan, J. B., Singer, R. A., Tschen, S.-I., Dhawan, S., Friel, J. M., Hipkens, S. B., Magnuson, M. A., Bhushan, A. and Sussel, L. (2011). Nkx2.2 repressor complex regulates islet β-cell specification and prevents β-to-α-cell reprogramming. *Genes Dev.* **25**, 2291-2305. doi:10.1101/gad.173039.111

Paroush, Z. (1994). Groucho is required for *Drosophila* neurogenesis, segmentation, and sex determination and interacts directly with hairy-related bHLH proteins. *Cell* **79**, 805-815. doi:10.1016/0092-8674(94)90070-1

Patel, S. R., Bhumbra, S. S., Paknikar, R. S. and Dressler, G. R. (2012). Epigenetic mechanisms of Groucho/Grg/TLE mediated transcriptional repression. *Mol. Cell* **45**, 185-195. doi:10.1016/j.molcel.2011.11.007

Romer, A. I., Singer, R. A., Sui, L., Egli, D. and Sussel, L. (2019). Murine perinatal β-cell proliferation and the differentiation of human stem cell-derived insulin-expressing cells require NEUROD1. *Diabetes* **68**, 2259-2271. doi:10.2337/db19-0117

Sander, M., Neubuser, A., Kalamaras, J., Ee, H. C., Martin, G. R. and German, M. S. (1997). Genetic analysis reveals that PAX6 is required for normal transcription of pancreatic hormone genes and islet development. *Genes Dev.* **11**, 1662-1673. doi:10.1101/gad.11.13.1662

Sander, M., Sussel, L., Conners, J., Scheel, D., Kalamaras, J., Dela Cruz, F., Schwitzgebel, V., Hayes-Jordan, A. and German, M. (2000). Homeobox gene Nkx6.1 lies downstream of Nkx2.2 in the major pathway of beta-cell formation in the pancreas. *Development* **127**, 5533-5540.

Santisteban, P., Recacha, P., Metzger, D. E. and Zaret, K. S. (2010). Dynamic expression of Groucho-related genes Grg1 and Grg3 in foregut endoderm and antagonism of differentiation. *Dev. Dyn.* **239**, 980-986. doi:10.1002/dvdy.22217

Scavuzzo, M. A., Hill, M. C., Chmielowiec, J., Yang, D., Teaw, J., Sheng, K., Kong, Y., Bettini, M., Zong, C., Martin, J. F. et al. (2018). Endocrine lineage biases arise in temporally distinct endocrine progenitors during pancreatic morphogenesis. *Nat. Commun.* **9**, 3356. doi:10.1038/s41467-018-05740-1

Sekiya, T. and Zaret, K. S. (2007). Repression by Groucho/TLE/Grg proteins: genomic site recruitment generates compacted chromatin in vitro and impairs activator binding in vivo. *Mol. Cell* **28**, 291-303. doi:10.1016/j.molcel.2007.10.002

Sosa-Pineda, B., Chowdhury, K., Torres, M., Oliver, G. and Gruss, P. (1997). The Pax4 gene is essential for differentiation of insulin-producing β cells in the mammalian pancreas. *Nature* **386**, 399-402. doi:10.1038/386399a0

Spaeth, J. M., Walker, E. M. and Stein, R. (2016). Impact of Pdx1-associated chromatin modifiers on islet β-cells. *Diabetes Obes. Metab.* **18** Suppl. 1, 123-127. doi:10.1111/dom.12730

Spaeth, J. M., Liu, J.-H., Peters, D., Guo, M., Osipovich, A. B., Mohammadi, F., Roy, N., Bhushan, A., Magnuson, M. A., Hebrok, M. et al. (2019). The Pdx1-Bound Swi/Snf chromatin remodeling complex regulates pancreatic progenitor cell proliferation and mature islet β-cell function. *Diabetes* **68**, 1806-1818. doi:10.2337/db19-0349

St-Onge, L., Sosa-Pineda, B., Chowdhury, K., Mansouri, A. and Gruss, P. (1997). Pax6 is required for differentiation of glucagon-producing α-cells in mouse pancreas. *Nature* **387**, 406-409. doi:10.1038/387406a0

Sussel, L., Kalamaras, J., Hartigan-O'Connor, D. J., Meneses, J. J., Pedersen, R. A., Rubenstein, J. L. R. and German, M. S. (1998). Mice lacking the homeodomain transcription factor Nkx2.2 have diabetes due to arrested differentiation of pancreatic beta cells. *Development* **125**, 2213-2221.

Tabula muris consortium, **Overall coordination**, **Logistical coordination**, **Organ collection and processing**, **Library preparation and sequencing**, **Computational data analysis**, **Cell type annotation**, **Writing group**, **Supplemental text writing group**, **Principal investigators.** (2018). Single-cell transcriptomics of 20 mouse organs creates a Tabula Muris. *Nature* **562**, 367-372. doi:10.1038/s41586-018-0590-4

Taylor, B. L., Liu, F.-F. and Sander, M. (2013). Nkx6.1 is essential for maintaining the functional state of pancreatic beta cells. *Cell Rep.* **4**, 1262-1275. doi:10.1016/j.celrep.2013.08.010

Turki-Judeh, W. and Courey, A. J. (2012). Groucho: a corepressor with instructive roles in development. *Curr. Top. Dev. Biol.* **98**, 65-96. doi:10.1016/B978-0-12-386499-4.00003-3

Villanueva, C. J., Waki, H., Godio, C., Nielsen, R., Chou, W.-L., Vargas, L., Wroblewski, K., Schmedt, C., Chao, L. C., Boyadjian, R. et al. (2011). TLE3 is a dual-function transcriptional coregulator of adipogenesis. *Cell Metab.* **13**, 413-427. doi:10.1016/j.cmet.2011.02.014

Wheat, J. C., Krause, D. S., Shin, T. H., Chen, X., Wang, J., Ding, D., Yamin, R. and Sweetser, D. A. (2014). The corepressor Tle4 is a novel regulator of murine hematopoiesis and bone development. *PLoS ONE* **9**, e105557. doi:10.1371/journal.pone.0105557

Yang, X., Graff, S. M., Heiser, C. N., Ho, K.-H., Chen, B., Simmons, A. J., Southard-Smith, A. N., David, G., Jacobson, D. A., Kaverina, I. et al. (2020). Coregulator Sin3a promotes postnatal murine β-cell fitness by regulating genes in Ca^{2+} homeostasis, cell survival, vesicle biosynthesis, glucose metabolism, and stress response. *Diabetes* **69**, 1219-1231. doi:10.2337/db19-0721

Yao, J., Lai, E. and Stifani, S. (2001). The winged-helix protein brain factor 1 interacts with groucho and hes proteins to repress transcription. *Mol. Cell. Biol.* **21**, 1962-1972. doi:10.1128/MCB.21.6.1962-1972.2001

Zhang, X., Chen, H.-M., Jaramillo, E., Wang, L. and D'Mello, S. R. (2008). Histone deacetylase-related protein inhibits AES-mediated neuronal cell death by direct interaction. *J. Neurosci. Res.* **86**, 2423-2431. doi:10.1002/jnr.21680

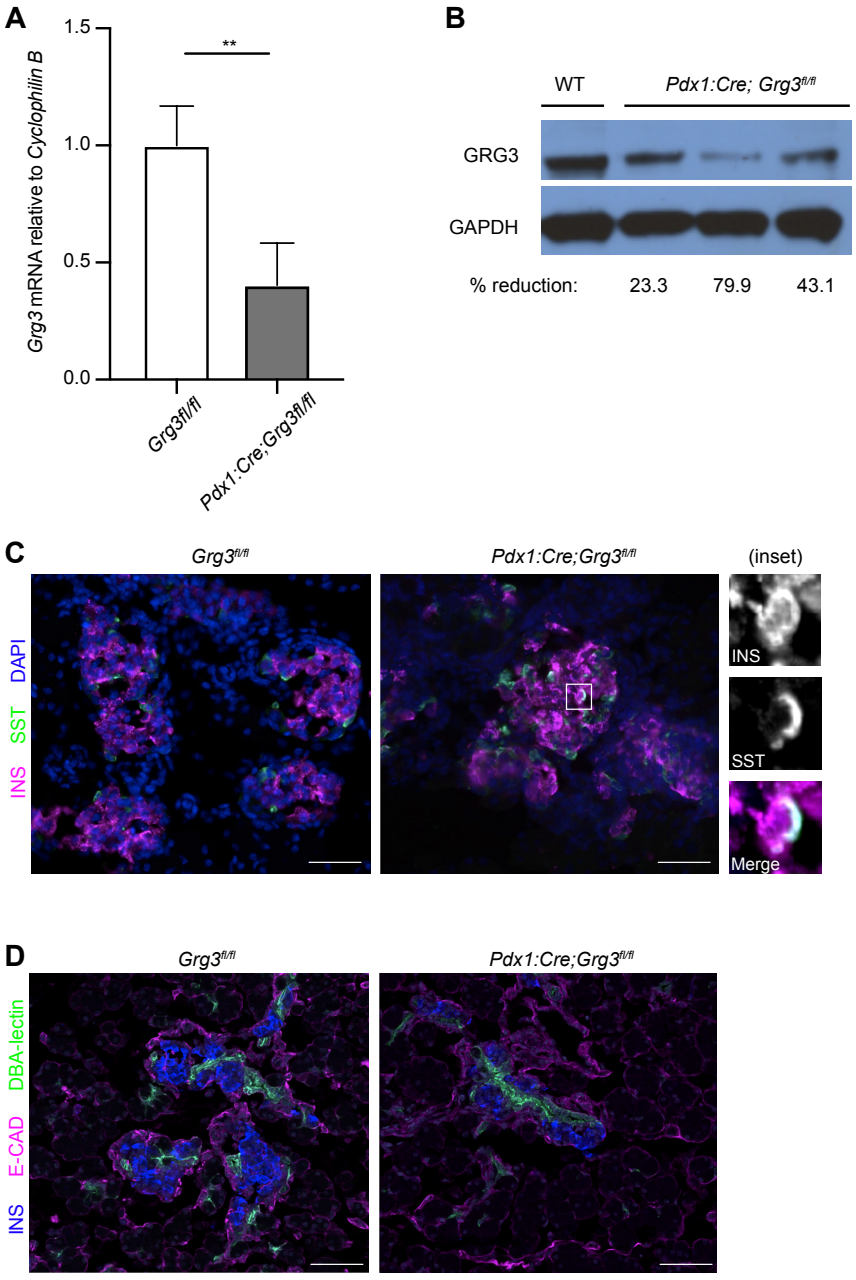

Figure S1. Validation of pancreas-specific *Grg3* knockout.

(A) *Grg3* mRNA levels are decreased in 8 week isolated islets from *Pdx1:Cre; Grg3*$^{fl/fl}$ mutants as measured by qPCR. n = 3 for each genotype. **P≤0.01; two-tailed student's t-test. (B) Western blot of protein from P0 pancreata showing reduction of GRG3 protein in *Pdx1:Cre; Grg3*$^{fl/fl}$ animals. (C) Immunofluorescent staining of 6 week *Pdx1:Cre; Grg3*$^{fl/fl}$

Development • Supplementary information

islets hormones. Inset shows example of bihormonal INS+/SST+ cell in *Pdx1:Cre; Grg3*$^{fl/fl}$ animal. Scale bars = 50 μm. (D) Immunofluorescent staining of E-cadherin and DBA-lectin of P0 *Grg3* single knockouts showing no visible defects in delamination of the endocrine population. Scale bars = 50 μm.

Development • Supplementary information

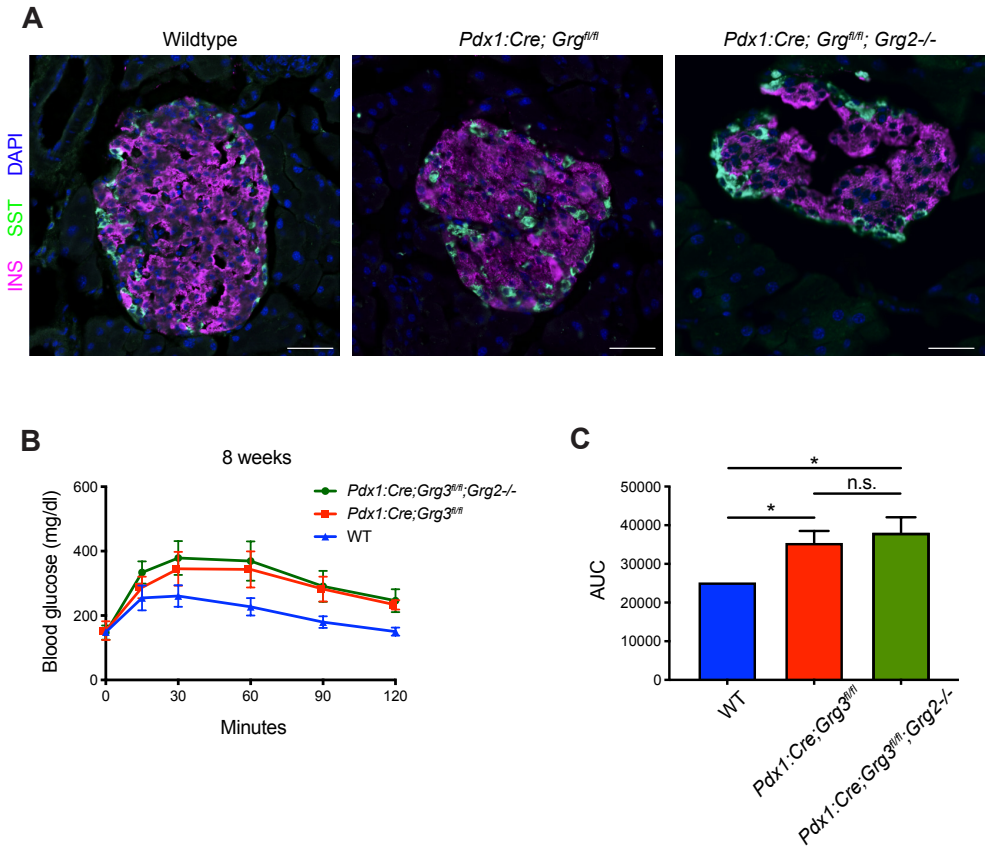

Figure S2. Loss of *Grg2* does not exacerbate *Grg3* knockout phenotype. (A) Immunofluorescent analysis of islets from 7 month control *Grg3* and *Grg2/3* knockout mice showing no visible worsening of the *Grg3* islet phenotype with additional loss of *Grg2*. Scale bars = 50 μm. (B) Glucose tolerance tests of 8 week *Grg3* and *Grg2/3* mutants. (C) AUC calculation of (B) showing no difference between *Grg3* and *Grg2/3* mutants. n = 4-6 for all genotypes. *P≤0.05; two-tailed student's t-test.

Development • Supplementary information

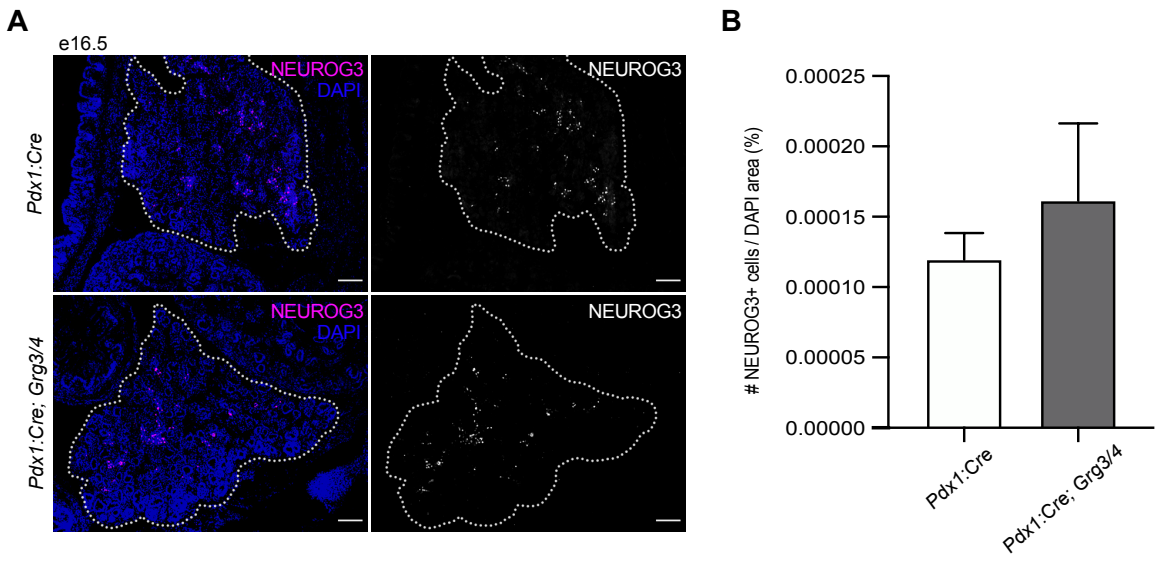

Figure S3. NEUROG3+ endocrine progenitors are unchanged in e16.5 *Pdx1:Cre; Grg3/4* mice.

(A) Immunofluorescent staining of e16.5 embryos for endocrine progenitor (NEUROG3+) population. Scale bars = 50 μm. (B) Quantification of NEUROG3+ cells in (A). n = 3 for each genotype.

Development • Supplementary information

A

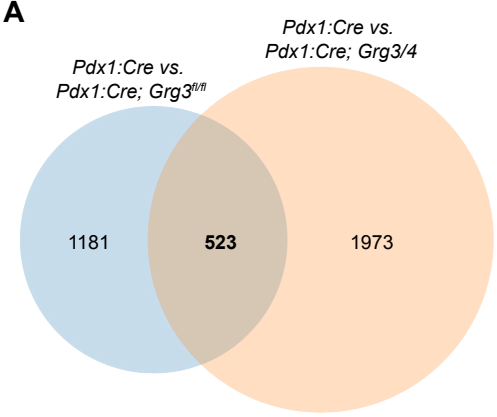

B

Downregulated genes from Fig 5C

	Pdx1:Cre vs. Pdx1:Cre; Grg3$^{fl/fl}$		*Pdx1:Cre vs. Pdx1:Cre; Grg3/4*	
Gene	**log2FC2**	**padj**	**log2FC**	**padj**
Npy	-0.93	0.1188	-2.56	1.62E-12
Ins2	-0.58	0.0216	-1.52	0.0015
Cpa1	-0.58	0.0692	-0.88	1.77E-21
Neurod1	-0.52	0.0165	-0.88	0.0027
Ins1	-0.47	0.1351	-1.43	0.0081
Mafa	-0.43	0.2477	-1.35	2.75E-14
Foxa2	-0.25	0.2985	-0.57	0.0009
Pdx1	-0.24	0.1980	-0.6	0.0002
Pax6	-0.18	0.5613	-0.52	0.0446
Rbpj	-0.08	0.8964	-1.09	1.53E-07
Pyy	0.25	0.3166	-0.71	3.27E-05
Ppy	0.30	0.3904	-0.55	0.0283

C

Upregulated genes from Fig 5D

	Pdx1:Cre vs. Pdx1:Cre; Grg3$^{fl/fl}$		*Pdx1:Cre vs. Pdx1:Cre; Grg3/4*	
Gene	**log2FC2**	**padj**	**log2FC**	**padj**
Fga	10.19	8.87E-08	10.44	3.19E-17
Fgg	9.38	8.91E-07	9.55	6.13E-15
Apoh	9.35	3.10E-05	9.5	4.09E-11
Foxa1	8.81	1.32E-28	8.77	2.11E-29
Hc	6.00	0.4511	8.42	7.31E-08
Bhmt	8.49	0.0049	8.25	0.0023
F11	7.26	0.3179	8.05	4.45E-07
Kng1	7.68	1.39E-06	7.98	2.84E-22
Ahsg	7.68	0.0081	7.83	0.0012
Kng2	5.71	0.0016	7.77	0.0003
Hsd3b3	5.73	0.4813	7.71	6.40E-06

Figure S4. Comparison of differentially expressed genes in *Pdx1:Cre; Grg3$^{fl/fl}$* vs. *Pdx1:Cre; Grg3/4* e18.5 pancreata.

(A) Venn diagram showing *Pdx1:Cre; Grg3/4* e18.5 pancreata have more differentially expressed genes than *Pdx1:Cre; Grg3$^{fl/fl}$* when compared to *Pdx1:Cre* controls. 523 genes are differentially expressed in both groups. (B) Select list of downregulated genes related to pancreas development and hormone expression from Fig. 5C including *Pdx1:Cre* vs *Pdx1:Cre; Grg3$^{fl/fl}$* comparison. Gray text indicates padj > 0.05 in the *Pdx1:Cre; Grg3$^{fl/fl}$* comparison. (C) Top 10 upregulated genes sorted by fold change including *Pdx1:Cre* vs *Pdx1:Cre; Grg3$^{fl/fl}$* comparison. Gray text indicates padj > 0.05 in the *Pdx1:Cre; Grg3$^{fl/fl}$* comparison.

Development • Supplementary information

A

	Gene	log2FC	padj
Acinar	*Cel*	-0.77	7.88E-15
	Cela1	-0.69	7.45E-11
	Cela2a	-0.43	0.0005
	Cela3b	-0.33	0.0120
	Cpa1	-0.88	1.77E-21
	Cpa2	-0.47	5.10E-06
	Cpb1	-0.94	3.61E-13
	Ctrb1	-0.51	5.53E-06
	Ctrc	*-0.05*	*0.9143*
	Ctrl	-2.69	1.01E-141
	Klk1	-1.23	0.0039
	Klk1b3	*-0.08*	*0.8825*
	Klk1b4	*-0.51*	*0.4180*
	Klk1b5	-1.04	2.35E-05
	Pnlip	*-0.14*	*0.8879*
	Pnliprp1	-0.44	7.37E-05
	Pnliprp2	-1.25	5.29E-33
	Prss1	-3.03	1.33E-103
	Prss2	*-0.22*	*0.2787*
	Prss3	-2.44	8.86E-104
	Rnase1	-1.05	3.10E-25
	Serpinb1a	-0.47	9.92E-05
	Serpini2	-1.08	5.28E-10
	Try10	-0.82	5.31E-14
	Try4	-1.16	4.28E-54
	Try5	-0.43	0.0317
Duct	*Muc1*	-0.46	6.56E-06
	Ptf1a	0.02	0.9292
	Hnf1b	0.43	0.4888
	Sox9	-0.20	0.4124
	Krt19	-0.07	0.8622

B

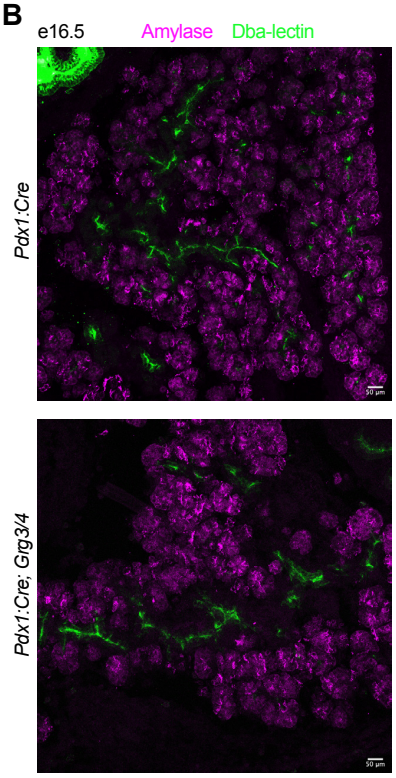

Figure S5. Overall pancreas morphology appears unaffected by loss of *Grg3/4*.

(A) List of acinar and duct genes from e18.5 RNA-seq analysis of *Pdx1:Cre* vs *Pdx1:Cre; Grg3/4* pancreata. Gray text indicates padj > 0.05 in the *Pdx1:Cre; Grg3*$^{fl/fl}$ comparison. (B) Immunofluorescent analysis of acinar (amylase) and duct (Dba-lectin) tissue e16.5 pancreata from control and *Pdx1:Cre; Grg3/4* mice showing no visual differences between genotypes. Scale bars = 100 μm.

Development • Supplementary information

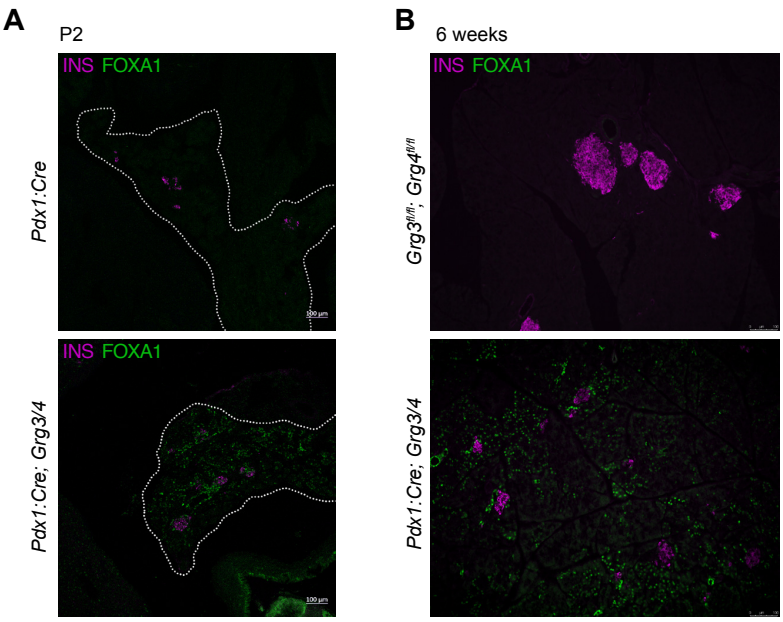

Figure S6. FOXA1 protein is maintained through 6 weeks of age in *Pdx1:Cre; Grg3/4* mutants.

(A) Immunofluorescent staining of P2 pancreata for INS and FOXA1 showing ectopic expression of FOXA1 in the pancreas of *Pdx1:Cre; Grg3/4* mutants. Scale bars = 100 μm. (B) Immunofluorescent staining of 6 week pancreata as in (A), showing ectopic FOXA1 protein maintained through 6 weeks of age. Scale bars = 100 μm.

Development • Supplementary information

Table S1. Differentially expressed *Foxa1* targets in e18.5 *Pdx1:Cre; Grg3/4* mutant pancreata.

Click here to Download Table S1

Table S2. Primers used for mouse genotyping.

Primer name	Sequence
Pdx1Cre_FWD	5'-CTG GAC TAC ATC TTG AGT TGC-3'
Pdx1Cre_REV	5'-GGT GTA CGG TCA GTA AAT TTG-3'
GenCre_FWD	5' CTG CCA CGA CCA AGT GAC AGC 3'
GenCre_REV	5' CTT CTC TAC ACC TGC GGT GCT 3'
Grg2WT_FWD	5' GGG ATT CTA GGA TTC TAG GCA GGG C 3'
Grg2WT_REV	5' TTG AGG CAT GGT CTT GCT TTG TAG C 3'
Grg2KO_FWD	5' GCA GCC TCT GTT CCA CAT ACA CTT CA 3'
Grg2KO_REV	5' AGA GCC AGG AAG ATG GTT CAG TTG G 3'
Grg3flox_FWD	5' GCT CCC TTC TTC AGC TTC CT 3'
Grg3flox_REV	5' GCT CCA AGA GGG ATT TTT AT 3'
Grg4flox_FWD	5' AGA AAT GCA GCC CAG AGT AA 3'
Grg4flox_REV	5' GGA GAC TTG GAA AAC GCT GA 3'

Development • Supplementary information

Table S3. Antibodies used for immunofluorescence and western blotting.

Target	Company/Source	Catalog #	Host species	Concentration
Alpha1 antitrypsin (AAT)	Thermo Fisher	PA5-16661	Rabbit	1:250
DAPI	Thermo Fisher	D1306	NA	1:1000
DBA-lectin, fluorescein	Vector	FL-1031	NA	1:100
E-cadherin	BD Biosciences	610182	Mouse	1:100
Foxa1	Sigma	HPA050505	Rabbit	1:200
GAPDH	Abcam	ab9485	Rabbit	1:1000 (WB)
Glucagon	Cell Signaling Technologies	2760S	Rabbit	1:500
Insulin	Dako/Agilent	IR00261-2	Guinea pig	1:1000
Ki67	Abcam	Ab15580	Rabbit	1:500
Neurod1	Sigma	HPA003278	Rabbit	1:200
Neurogenin3	From C. Wright	NA	Rabbit	1:200
Pdx1	Abcam	ab47308	Guinea pig	1:500
Somatostatin	Santa Cruz	sc-47706	Rat	1:500
TLE3 (Grg3)	Santa Cruz	sc-9124	Rabbit	1:100 (WB)
488 anti-guinea pig	Thermo Fisher/Invitrogen	A11073	Goat	1:500
555 anti-guinea pig	Thermo Fisher/Invitrogen	A21435	Goat	1:500
488 anti-rabbit	Thermo Fisher/Invitrogen	A21206	Donkey	1:500
594 anti-rabbit	Thermo Fisher/Invitrogen	A21207	Donkey	1:500
647 anti-rabbit	Thermo Fisher/Invitrogen	A21244	Goat	1:500
647 anti-rat	Thermo Fisher/Invitrogen	A21247	Goat	1:500

Development • Supplementary information

Table S4. Taqman probes used for RT-qPCR

Gene name	Company	Catalog number
Chga	ThermoFisher	Mm00514341_m1
Cyclophilin B	ThermoFisher	Mm00478295_m1
Ecad	ThermoFisher	Mm01247357_m1
Gcg	ThermoFisher	Mm00514341_m1
Grg2	ThermoFisher	Mm00498094_m1
Grg3	ThermoFisher	Mm00437097_m1
Grg4	ThermoFisher	Mm01195172_m1
Ins1	ThermoFisher	Mm00801712_m1
Ins2	ThermoFisher	Mm00801712_m1
PP	ThermoFisher	Mm00435889_m1
Sst	ThermoFisher	Mm00436671_m1

Development • Supplementary information